

Review

# Advances in Shape Memory Alloy-Based Reinforcement in Steel Structures: A Review

Chenxi Shao and Yonghui Huang \* 

Research Center of Wind Engineering and Engineering Vibration, Guangzhou University,  
Guangzhou 510006, China; shaocx@e.gzhu.edu.cn

\* Correspondence: huangyh@gzhu.edu.cn; Tel.: +86-159-2038-3318

**Abstract:** The utilization of shape memory alloys (SMAs) to reinforce steel structures has been proven to be an efficient and reliable method, the structural strengthening needs can be met without the need for tensioning equipment by activating the SMAs to generate restoring stresses. This paper firstly introduces the properties of SMA, and then presents the latest research progress, opportunities and challenges of SMA in the field of steel structural reinforcement, both in terms of basic components and applications. In terms of components, the construction forms and working mechanisms of Fe-SMA strips, SMA/CFRP composite patches and SMA dampers are introduced. On this basis, the application of SMA in steel structures reinforcement is introduced, and its effect is analyzed from three aspects: crack restoration, seismic retrofitting and structural strengthening. Finally, the results of the current research are summarized and the shortcomings are analyzed, hoping to provide a reference for the research of SMA in the field of steel structures reinforcement.

**Keywords:** steel structure; shape memory alloy (SMA); shape memory effect; mechanical properties; structure reinforcement

## 1. Introduction

The United States Federal Highway Administration has shown that fatigue is one of the main causes of steel structure failure, and more than 80% of steel structures fail due to fatigue [1]. Moreover, fatigue is typically catastrophic to the structure and can result in significant economic and human losses [2,3]. Therefore, in order to ensure that steel structures are able to withstand anticipated loads, stresses, and environmental conditions during their intended lifespan, the health of the steel structure needs to be monitored, and damaged structures need to be reinforced. Traditional reinforcement methods, including crack-stopping holes, adding steel plates, welding, etc. [4], can be used to strengthen structures, but they have some disadvantages, such as increased weight, difficulty in their application, and susceptibility to corrosion and fatigue damage [5]. Therefore, research for more efficient and economical reinforcement techniques has been a popular area of civil engineering in recent years [6].

Shape memory alloys (SMAs), as a new smart material, have been widely used in medical and aerospace applications [7–10]. In recent years, they have also been introduced into the field of civil engineering by many scholars due to their cost-effectiveness and unique properties. One of the highlights is the research and development of various SMA-based components and devices. In addition, many scholars have introduced SMA into the field of structural reinforcement [11–14]. After thermal activation, SMAs can realize the active control of structural stiffness and deformation, as well as repair the local damage and cracks of structures. Due to SME, no complex tensioning equipment is required to realize the state of pretension, which eliminates the restriction on operating spaces and improves the convenience of construction. This paper takes the SMA-based reinforcement in steel structures as the theme and reviews the research results, opportunities, and challenges at the present



**Citation:** Shao, C.; Huang, Y. Advances in Shape Memory Alloy-Based Reinforcement in Steel Structures: A Review. *Buildings* **2023**, *13*, 2760. <https://doi.org/10.3390/buildings13112760>

Academic Editor: Hiroshi Tagawa

Received: 29 September 2023

Revised: 19 October 2023

Accepted: 25 October 2023

Published: 1 November 2023



**Copyright:** © 2023 by the authors. Licensee MDPI, Basel, Switzerland. This article is an open access article distributed under the terms and conditions of the Creative Commons Attribution (CC BY) license (<https://creativecommons.org/licenses/by/4.0/>).

stage from three aspects, namely the properties of SMAs, SMA-based components, and technology, as well as the application of SMA-based reinforcement, in the hopes of providing references for further research on SMAs in the field of steel structure reinforcement.

## 2. Research Significance

Structures in service will inevitably produce cracks and other fatigue damage, which not only affects the suitability and durability of the structure, but also affects the safety of the structure. Therefore, research on more effective and economical structural reinforcement techniques to ensure the safety and functional requirements of existing structures in service is of great significance for the stable development of society. The new reinforcement technology with integrated smart materials (SMAs) has good potential for application in the field of structural reinforcement due to its advantages, such as being lightweight and the minimal construction required. This paper reviews the properties of SMAs and their application in the field of structural steel reinforcement with respect to the current year, with the aim of providing a background of their significance for further research in this field.

## 3. Material Properties of SMAs

Low-temperature stable martensite and high-temperature stable austenite are the two main phases of SMAs, and the fundamental characteristic of an SMA is the reversible transition between martensite and austenite [15]. Additionally, SMAs will exhibit the shape memory effect and the superelastic effect through different triggering mechanisms. These two effects and the damping effects are the main reasons why SMAs are used in civil engineering [16].

### 3.1. Shape Memory Effect

The shape memory effect is the ability of a deformed SMA to return to its initial shape after a certain thermal activation. The characteristic temperatures of the shape memory effect include the following:

- (1)  $A_s$  (Austenite Start Temperature): The temperature at which the transformation of martensite to austenite starts.
- (2)  $A_f$  (Austenite Finish Temperature): The temperature of the full transformation of martensite to austenite.
- (3)  $M_s$  (Martensite Start Temperature): The temperature at which the transformation of austenite to martensite initiates.
- (4)  $M_f$  (Martensite Finish Temperature): The temperature at which austenite fully transforms to martensite.

The phase transition temperatures of SMAs can be obtained via the differential scanning calorimetry (DSC) tests. Figure 1 shows the shape memory effect of SMAs. It should be noted that an SMA transforms from twinned martensite to detwinned martensite under stress at temperatures below the  $M_f$ , and the deformation of the SMA does not disappear completely with the disappearance of the stress (with residual deformation). However, the detwinned martensite will transform into austenite if the material is heated above the  $A_f$ . On this basis, the SMA changes again from austenite to twinned martensite by lowering the temperature below the  $M_f$ . At this point, the deformation of the SMA is fully restored (residual deformation disappears).

### 3.2. Superelastic Effect and Damping Effect

While the aforementioned shape memory effect is induced by temperature, the next superelastic effect is induced by stress at a constant temperature greater than the  $A_f$ . The characteristic stresses of the superelastic effect include  $\sigma_{As}$ ,  $\sigma_{Af}$ ,  $\sigma_{Ms}$ , and  $\sigma_{Mf}$ , which can be extracted from the stress–strain response obtained in cycling loading tests.

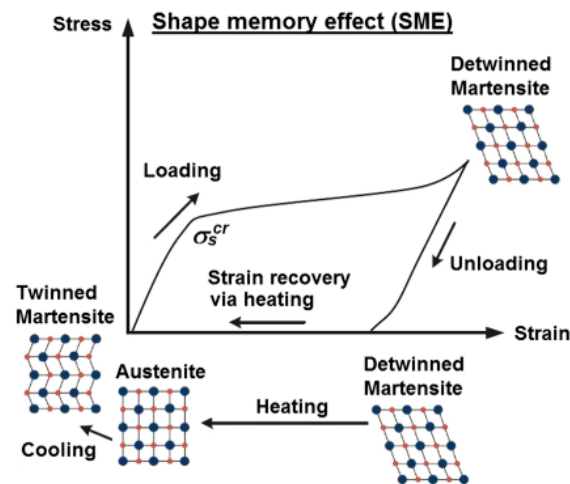


Figure 1. Shape memory effect of SMAs, reproduced with permission from [16], Elsevier, 2019.

Figure 2 shows the superelastic effect of SMAs. It can be seen that the initial state of the SMA is austenite. The SMA starts martensitic transformation when the loading stress reaches  $\sigma_{Ms}$ , at which time the Young's modulus of the SMA is significantly reduced. Subsequently, when the loading stress reaches  $\sigma_{Mf}$ , the SMA finishes the martensitic transformation into the hardening stage. It is worth noting that when the SMA enters the hardening stage, its Young's modulus increases significantly. On this basis, the SMA transforms from martensite to austenite when the stress is unloaded to  $\sigma_{As}$ . And the SMA finishes the transformation from martensite to austenite when the stress is unloaded to  $\sigma_{Af}$ . Finally, when the stress disappears, the deformation of SMA automatically recovers completely, and its recoverable strain is as high as 8%~10%. In addition, it should be noted that the above loading and unloading cycles form hysteresis loops, resulting in the dissipation of energy, which is the damping effect of the SMA.

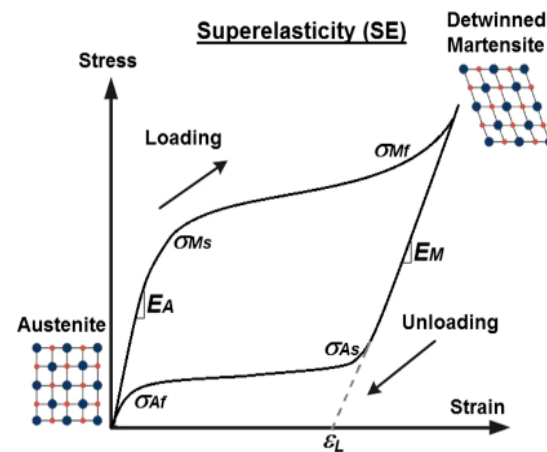


Figure 2. Superelastic effect of SMA, reproduced with permission from [16], Elsevier, 2019.

## 4. Mechanical Properties of SMAs

### 4.1. Basic Mechanical Properties

Currently, dozens of shape memory alloys have been discovered, the most valuable of these in civil engineering are Cu-based SMAs, iron-based SMAs (Fe-SMAs), and Ni-Ti SMAs [17]. The key characteristics of SMAs commonly used in civil engineering are shown in Table 1.

**Table 1.** Key characteristics of SMAs.

Alloy	Elastic Modulus (GPa)	$\sigma_{Ms}$ (MPa)	Recovery Strain (%)	$A_f$ (°C)	Type	Reference
Ni <sub>50.02</sub> -Ti <sub>49.98</sub>	62.5	401	6	−10	Wire, cable, bar, plate, spring	[15,18]
Ni <sub>50.5</sub> -Ti <sub>49.5</sub>	45.3	—	4.6	53		[19]
Ni <sub>47.45</sub> -Ti <sub>37.86</sub> -Nb <sub>14.69</sub>	20	250	3.2	22		[20]
Cu <sub>71.9</sub> -Al <sub>16.6</sub> -Mn <sub>9.3</sub>	31.2	210	7	−39	Wire, cable, bar	[21]
Cu <sub>87.68</sub> -Al <sub>11.7</sub> -Be <sub>0.62</sub>	32	230	2.4	−65		[22]
Fe <sub>17</sub> -Mn <sub>5</sub> -Si <sub>10</sub> -Cr <sub>4</sub> -Ni <sub>1</sub> -V <sub>C63</sub>	165	396	3.5	162		[23]

It can be seen that Ni-Ti SMAs and Cu-based SMAs have a lower  $A_f$  (austenite at room temperature) and higher recovery strains, so they are often used to improve the limited-displacement and re-centering capabilities of structures via the superelasticity effect [24]. Fe-SMAs are often used to strengthen structures via the shape memory effect [25]. In addition, alloys with different chemical compositions have different transformation temperatures. The transformation temperatures are important parameters for SMAs and determine whether they exhibit superelasticity or shape memory effects in the working environment. Therefore, in practical applications, SMAs of different compositions should be purchased from material suppliers according to the working environment [16,26].

#### 4.2. Cycling Loading

##### 4.2.1. Comparison of Different Elements of SMAs

The typical cyclic stress–strain responses of SMAs with different elements are shown in Figure 3. It can be seen that NiTi-SMAs have better self-centering ability, limiting ability, and energy dissipation ability. In addition to this, as mentioned before, NiTi has a low  $A_f$  (which can exhibit sufficient superelasticity), so NiTi-SMAs are often used to develop new types of isolators or dampers [26].

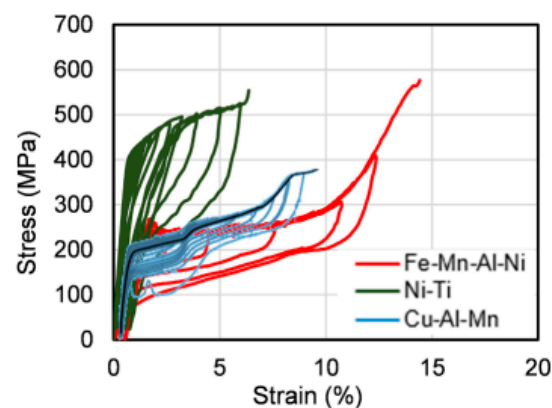


**Figure 3.** Stress–strain responses of SMAs with different elements, reproduced with permission from [27], Elsevier, 2019.

##### 4.2.2. Effect of Annealing on Mechanical Properties of SMAs

Annealing affects the mechanical properties of SMAs, and different temperatures and durations have different effects on the mechanical properties of SMAs. In order to investigate the effect of annealing on the mechanical properties of SMAs, a series of NiTi-SMA bars were subjected to different annealing schemes and cyclic tensile tests; an overview of the tests is shown in Figure 4.

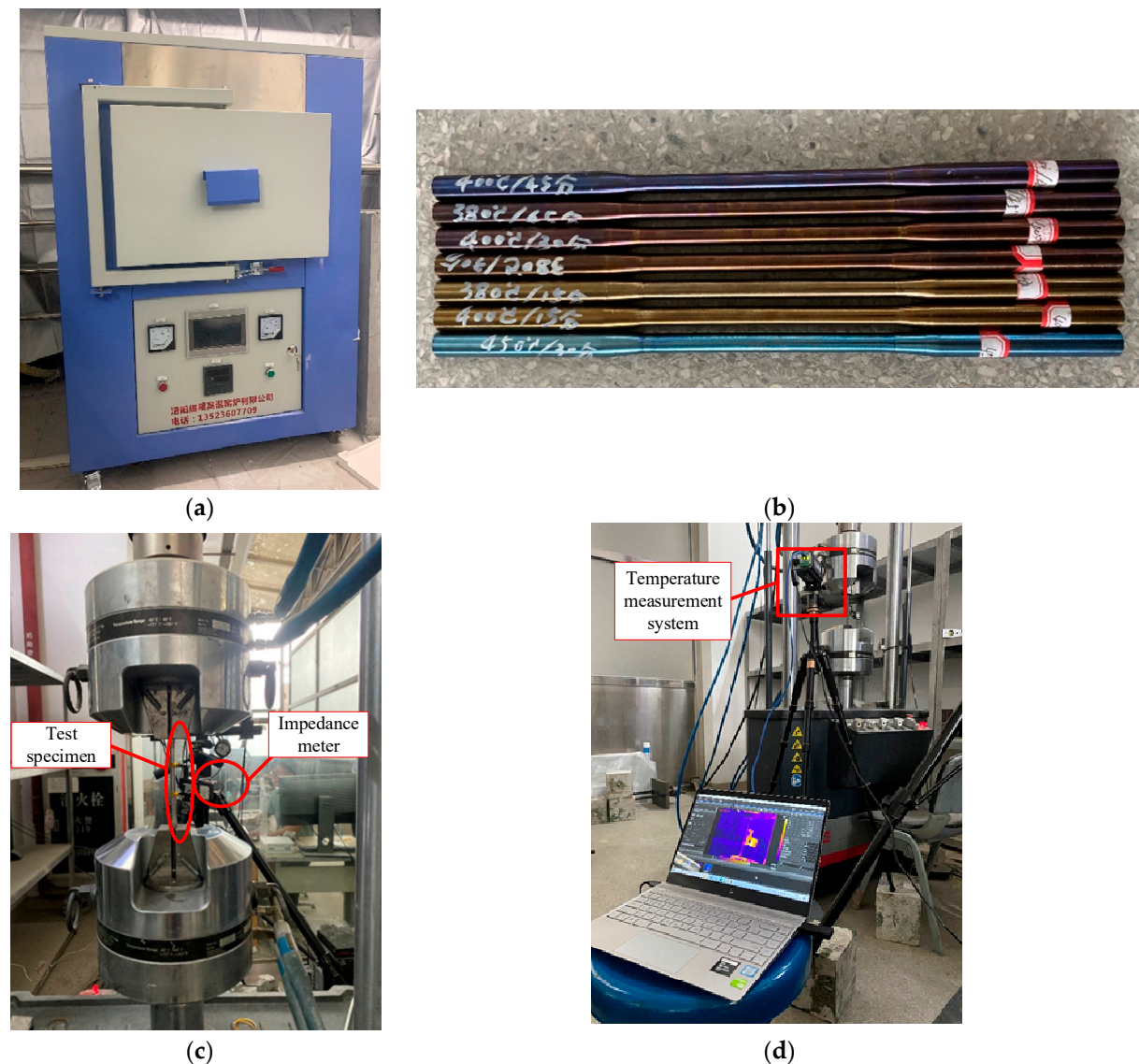


**Figure 4.** Overview of the tests: (a) muffle furnace; (b) annealed SMA bars; (c) MTS; (d) temperature monitoring.

The test results are shown in Figure 5. It can be seen that the residual displacement of the unannealed specimen is significantly larger than that of the annealed specimen, and its maximum residual strain is as high as 3.3%. In addition, after unloading for a period of time, the deformation of the annealed specimen is fully recovered, while the unannealed specimen still has a small residual strain.

At the same annealing temperature, the superelasticity and energy dissipation capacity of the specimen increase with an increasing annealing time, and its residual strain decreases. For example, the residual strain of the specimen annealed at 350 °C for 30 min is 50% lower than the residual strain of the specimen annealed at 350 °C for 15 min. At the same annealing time, the superelasticity of SMA becomes stronger with the increase in the annealing temperature, but the superelasticity of SMAs will deteriorate when the temperature exceeds a certain value. For example, the superelasticity of the specimen annealed at 380 °C for 30 min is significantly higher than that of the specimen annealed at 400 °C for 30 min. However, the superelasticity of the specimen annealed at 450 °C for 30 min is significantly lower than that of the specimen annealed at 400 °C for 30 min. Frick et al. [28] confirmed that excessively high annealing temperatures can have a deteriorating effect on the strain-recovery characteristics of SMAs.

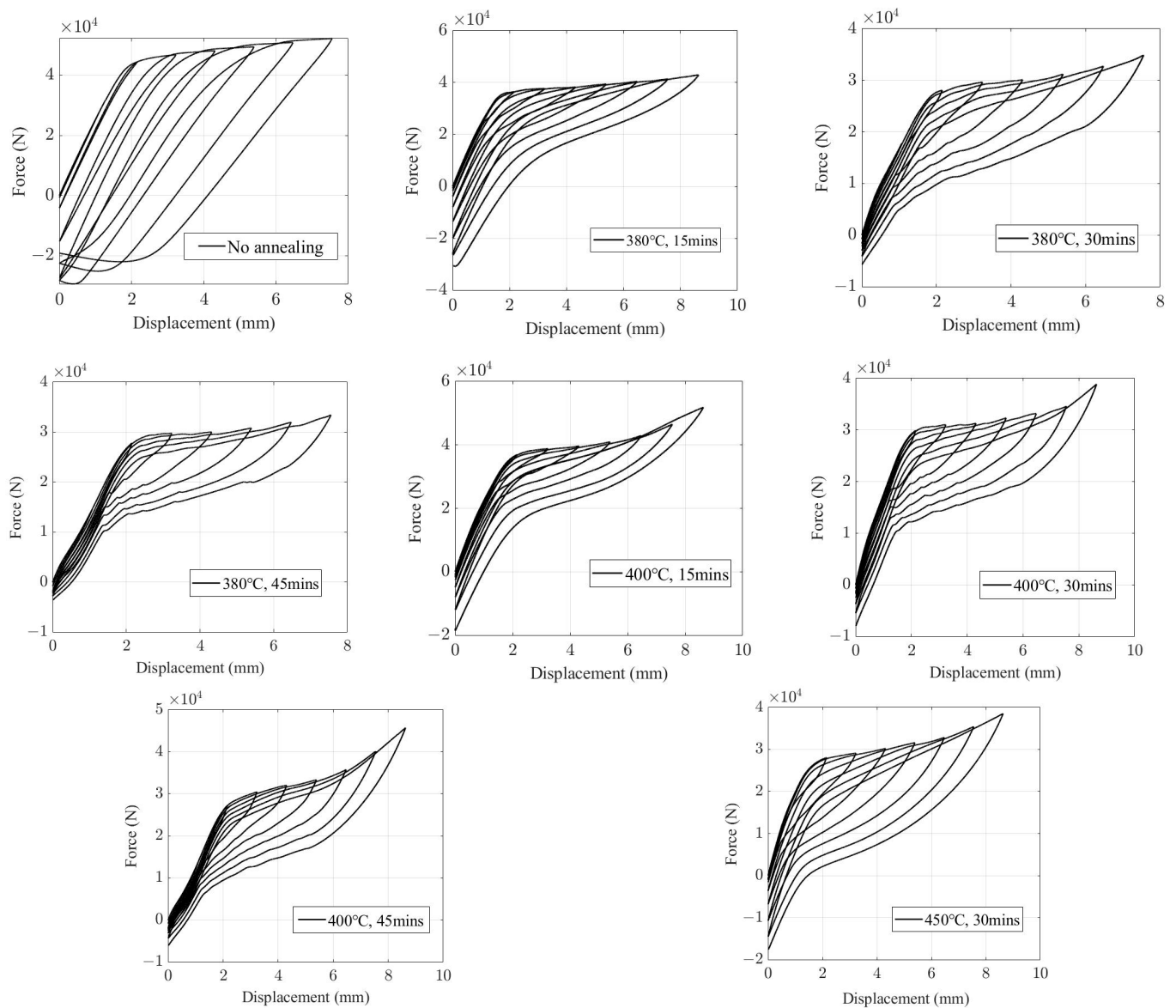


**Figure 5.** Force-displacement responses of NiTi-SMA bars under different annealing schemes.

It is worth noting that annealing also changes the transformation temperature of SMAs. Therefore, in addition to adjusting the chemical composition of the SMA, as described in the previous section, the transformation temperature of the SMA can be made to meet the demands of the working environment through annealing. The former approach can be performed by material suppliers (material engineers), and civil engineers are capable of performing the latter.

#### 4.2.3. Fatigue Properties

SMAs have excellent fatigue properties and their fatigue life can reach  $10^3$ – $10^7$  cycles, depending on the strain range/amplitude, and finally fractures just like any other engineering materials [29–34]. In addition, Lin et al. [35] investigated the effect of temperature on the fatigue performance of SMAs and experimentally studied the fatigue life of SMAs at four temperatures with different strain amplitudes; the results of the experiment are shown in the Figure 6. It can be seen that both temperature and strain amplitude have an effect on the fatigue life of SMAs. At the same temperature, the fatigue life of SMAs decreases with the increase in the strain amplitude, while at the same strain amplitude, the fatigue life of the SMA decreases with the increase in the temperature.

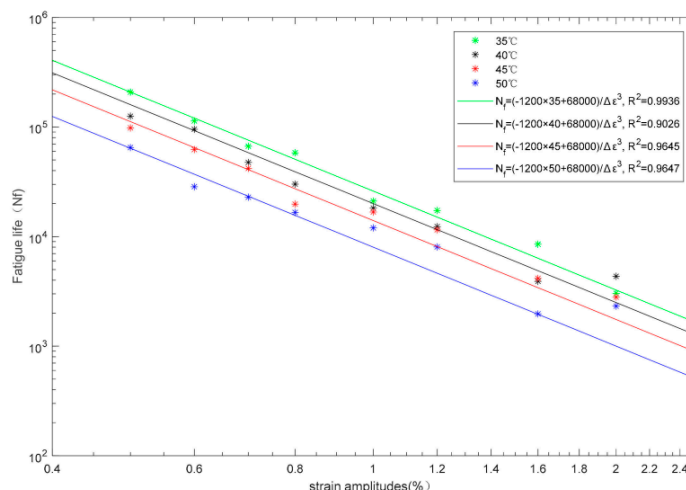


Figure 6. Fatigue life curves at different temperatures for various strain amplitudes [35].

### 5. SMA-Based Components and Technologies for Reinforced Steel Structures

Currently, many scholars are focusing on the development and research of new SMA-based components and devices and have already achieved more results. Representative components or devices in the field of reinforcement for steel structures include Fe-SMA strips, SMA/CFRP composite patches, and an SMA-based damper or brace.

#### 5.1. Fe-SMA Strip

##### 5.1.1. Reinforcement Mechanism

Fe-SMAs are often used to replace steel plates for structural reinforcement due to their low price, corrosion resistance, and stable mechanical properties [36–39]. Fe-SMA strips are commonly used components in the field of steel structural reinforcement, and the schematically illustrated strengthening procedures of Fe-SMA strips are shown in Figure 7 [40,41]. First, pre-straining was applied to the Fe-SMA strip (step 1), which was subsequently unloaded to a stress-free condition (step 2). Afterwards, the Fe-SMA strip, which was obtained from step 2, was connected to the steel beam (step 3) and heated until the temperature reached the  $A_f$  (step 4), and it was subsequently cooled (step 5). Due to the anchorage, the shape memory effect of the Fe-SMA strips is restricted (deformation of the strip is restricted), thus providing tensile stresses to the steel beam.

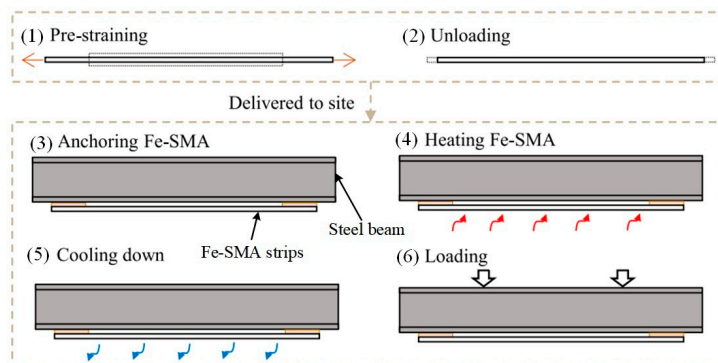


Figure 7. Strengthening procedures of steel beams using Fe-SMA strips, reproduced with permission from [40], Elsevier, 2023.

##### 5.1.2. Mechanical Properties

The method described above is known as the prior activation method and is often used to repair structural cracks and improve the bearing capacity of structures. The method has received much attention from scholars in recent years due to the convenience of applying pre-stress to the structure [42].

Fatigue properties are one of the most important reasons for determining whether a component can be used in a reinforced structure, so many scholars have conducted experimental studies on the fatigue performance of Fe-SMA strips. Ghafoori [43] studied the fatigue properties of Fe-SMA strips under high cyclic loading and proposed a safe design formula for Fe-SMA strips as pre-stressing elements. The experimental results show that Fe-SMA strips have very good fatigue properties. Marinopoulou et al. [44] conducted fatigue tests on Fe-SMA strips under pre-stressing conditions, and the recovered stress of Fe-SMA strips decreased by about 2% compared with that before the test. Hosseini et al. [45] investigated the effect of multiple thermal activations on the pre-stress of Fe-SMA strips and showed that although the pre-stress of Fe-SMA strips subjected to cyclic loading was reduced, it could be restored to its original level by means of secondary thermal activation. This shows that Fe-SMAs have very excellent fatigue properties, and they shall be considered in the design of structural reinforcements.

In addition to the fatigue properties, the pre-strain length and activation temperature of Fe-SMA strips have received much attention from scholars because they are related to the recovery stresses of Fe-SMA strips. Izadi et al. [46] found that the recovery stress of Fe-SMA strips could reach 430 MPa at the pre-strain of 2% and the activation temperature of 260 °C. More data on the recovery stresses of the Fe-SMA strips under different experimental conditions can be found in Table 2. It can be seen that the activation temperature of Fe-SMA strips is within 160–400 °C, which is acceptable for steel structures, but the activation temperature should not be too high for concrete structures, otherwise it may lead to the destruction of the mechanical properties of the concrete. In addition, the size and pre-strain of Fe-SMA strips have an effect on the optimal activation temperature, so the specific parameters of Fe-SMA strips and activation temperature should be determined through experiments in practical applications.

**Table 2.** Recovery stress of Fe-SMA strips under different experimental conditions.

Alloy	Size (mm)	Pre-Strain (%)	Activation Temperature (°C)	Recovery Stress (MPa)	Reference
Fe-17Mn-5Si-10Cr-4Ni-1Vc	0.7 × 3	4	225	380	[47]
		4	160	330	
	0.9 × 3	4	160	580	[48]
		4	160	266	[49]
	—	4	160	350	[50]
		2	160	372	[43]
	1.5 × 10	2	160	177~200	[51]
	1.7 × 25	2	160	406	[52]
0.8 × 52.5	2	160	292	[53]	
1.5 × 100	2	180	330		
Fe-28Mn-6Si-5Cr-0.53Nb-0.06C	—	4	397		[54]
Fe-28Mn-6Si-5Cr	—			255	[55]
Fe-18Mn-8Cr-4Si-2Ni-0.36Nb-0.36N		3	300	185	
Fe-Mn-Si alloy	1.5 × 20	2	160	308	[56]
		4	160	348	
	1.5 × 15.8	≈3	155	268~295	[57]

### 5.1.3. Connection and Activating Methods

A reliable connection between Fe-SMA strips and parent steel components is required when strengthening structures. Connecting methods that have been proposed include bolt anchorage, nail-anchor, friction clamp, and adhesive bonding [46,58–60], as shown in Figure 8 [61].

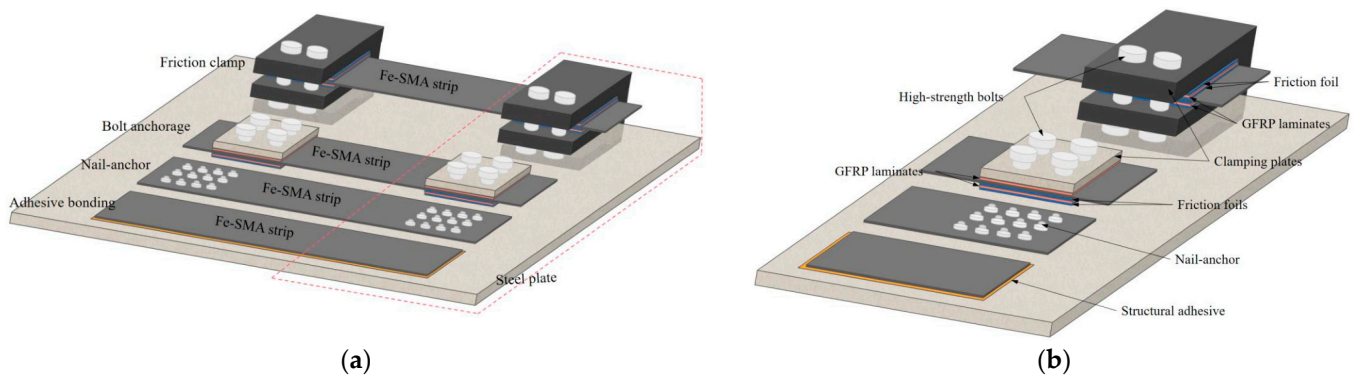


**Figure 8.** Connection methods between steel plate and Fe-SMA strips [61]: (a) reinforcing of steel plates; (b) configuration details.

Izadi et al. [52] proposed a mechanical anchorage system for the anchoring of Fe-SMA strips to steel plates or steel beams (as shown in Figure 9) and verified the effectiveness of the system using fatigue tests. The results show that the parent structure under this system has better integrity with the Fe-SMA strips, and the Fe-SMA strips exhibit very excellent fatigue performance. Fritsch et al. [62] used nails to anchor Fe-SMA strips to steel beams and experimentally analyzed the effectiveness of different nails and their distributions. Wang and Li [63–65] proposed a two-component epoxy adhesive SikaPower-1277 to bond the parent structure with Fe-SMA strips in order to minimize the damage of the parent steel structure. Furthermore, thermal activation methods for Fe-SMAs include a flame-spraying gun, infrared heating, electric heating furnace, electric ceramic, and electrical resistance heating [51,66–68]. It is worth noting that although nail and bolt anchors have the advantage of being stronger, damage to the parent structure due to anchoring is unavoidable. Therefore, when selecting the choice of an anchoring method adhesive bonding and friction clamps should first be considered.

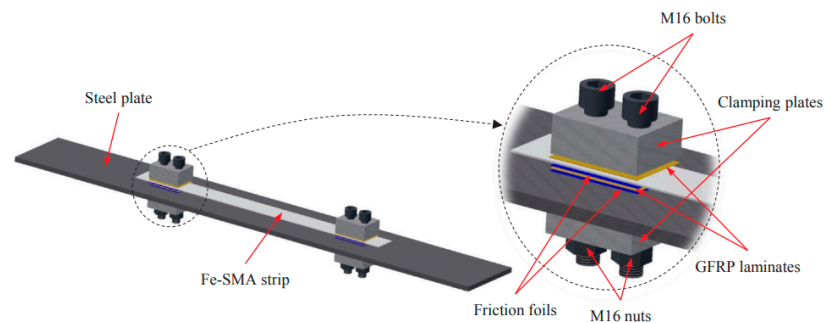


**Figure 9.** Components of the mechanical anchorage system developed for SMA-to-steel joints reproduced with permission from [52], Elsevier, 2018.

## 5.2. SMA/CFRP Composite Patch

### 5.2.1. Reinforcement Mechanism

The effectiveness of pre-stressed Carbon Fiber Reinforced Polymer (CFRP) panels for reinforcing steel structures has been demonstrated by a number of studies [69–73], but how to conveniently apply pre-stress is a big challenge. To solve this problem, some scholars have proposed the concept of SMA/CFRP composite patches [74]; NiTi-SMA wires are frequently employed in these studies, and the term “SMA wire” refers to an NiTi-SMA wire, unless specified otherwise. The fabrication and reinforcement procedures for SMA/CFRP composite patches are shown in Figure 10 [75,76]. First, pre-straining was applied to the SMA wires (step 1), which was subsequently unloaded to a stress-free condition (step 2). Afterwards, the SMA wires, which were obtained from step 2, and CFRP materials were glued together to form the SMA/CFRP composite patches (step 3). Then, the SMA/CFRP

composite patch was anchored to the steel beam and heated until the temperature reached the  $A_f$  (step 4) and subsequently cooled (step 5).

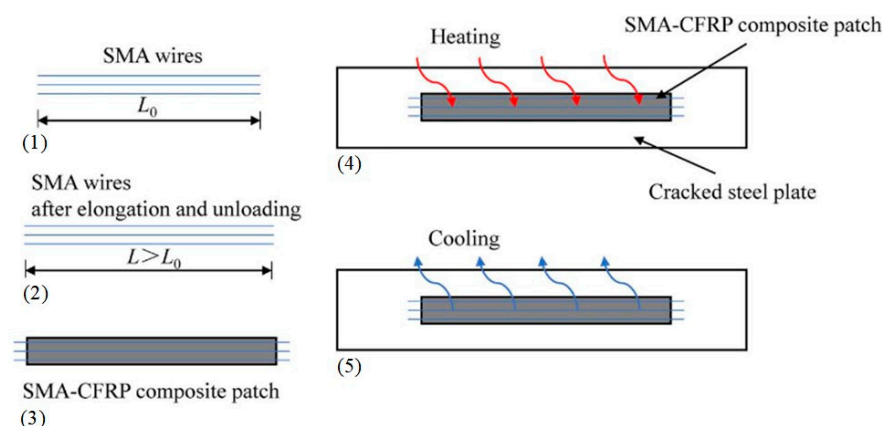


**Figure 10.** Fabrication and reinforcement procedures for the SMA/CFRP composite patch, reproduced with permission from [75], American Society of Civil Engineers, 1997.

Currently, there are two types of SMA/CFRP composite patches, with one as shown in Figure 10, where the SMA is fully composite with the CFRP by means of a bonding adhesive. The patch can only be heated by an electric current, and the heat resistance of the bonding adhesive needs to be considered. The other is shown in Figure 11; the advantage of this system is that the activation section is exposed and the heat resistance of the epoxy resin does not need to be taken into account when heating the section [77,78].



**Figure 11.** SMA/CFRP composite pre-stressed strengthening system, reproduced with permission from [77], Elsevier, 2023.

### 5.2.2. Bonding Performance between SMA and CFRP

It can be seen that the SMA/CFRP composite patch does not require large tensioning equipment and its pre-stressing is applied to the structure using the shape memory effect of the SMA. However, effective bonding between the SMA and CFRP is a prerequisite for the patch to work properly. Currently, epoxy resins are commonly used as an adhesive between SMA and CFRP, and many studies have demonstrated their effectiveness [75,79–83]. Furthermore, Zheng et al. [84] bonded SMA wires to CFRP with an epoxy resin and experimentally investigated the bonding performance of the patches, and the results showed that a reasonable selection of the number of SMA wires could effectively avoid the debonding of the two. El-Tahan et al. [85] showed that for the patch, debonding can be effectively prevented by increasing the anchorage length between the SMA wire and CFRP. In addition, Gu et al. [86] pointed out that debonding between the SMA and CFRP in SMA/CFRP composite patches is the main reason for the degradation of their mechanical properties, and in order to solve this problem, they proposed the idea of fabricating new specimens with orthogonally embedded SMA wires and sandwiched two-dimensional SMA film lattices, which is expected to solve the debonding risk.

### 5.2.3. Mechanical Properties

In order to prove the effectiveness of this method, many studies have been conducted. Yang et al. [87] investigated the fracture behavior of SMA/CFRP composites using bending and Charpy impact tests. Their findings indicated that incorporating an SMA alloy

into conventional composites enhances the ductility and impact resistance of the hybrid composite. Gu et al. [86] showed that embedding SMA wires into CFRP can effectively improve the energy absorption capacity and toughness of CFRP. Abdy et al. [79] developed a self-pre-stressing CFRP/SMA composite patch and verified its effectiveness through tests, as shown in Figure 12. The results demonstrated that it can be used as simple and effective solutions to significantly enhance the fatigue life of cracked steel structures. Furthermore, El-Tahan et al. [88] proposed an SMA/CFRP composite patch and investigated its fatigue properties experimentally, which showed that the patch retained more than 80% of its pre-stress after undergoing 2 million loadings. Deng et al. [89] also compared an SMA/CFRP composite patch, CFRP sheet, and SMA patch reinforcement through experiments, and the results showed that the SMA/CFRP composite patch was better. Russian et al. [90] investigated the effect of surface preparation on the effectiveness of SMA/CFRP composite patches for reinforcing steel structures. The results show that smoother steel surfaces resulted in less effective reinforcement with SMA/CFRP composite patches.

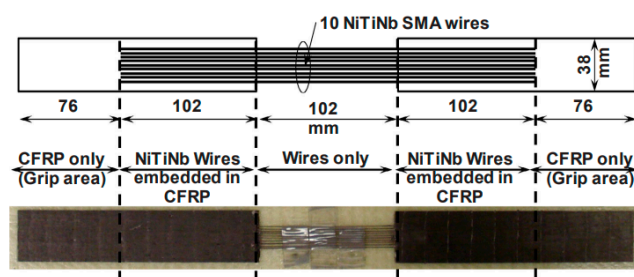


**Figure 12.** SMA/CFRP composite patch, which was developed by Abdy, reproduced with permission from [79], Elsevier, 2018.

### 5.3. SMA-Based Damper and Brace

SMA dampers can provide stiffness and are usually used in conjunction with an anti-lateral brace. SMA dampers typically utilize the superelastic and damping effects of the SMA to provide energy dissipation to a structure while reducing its lateral displacement and providing the ability of self-centering [91,92]. Liu et al. [93] designed a tension-compression SMA damper and obtained its characteristic parameters through tests. The experimental results demonstrated the distinct effectiveness of SMA dampers in reducing the displacement and acceleration responses of structures. Han et al. [94] proposed an NiTi-SMA wires-based damper capable of tension, compression, and torsion simultaneously. Qiu et al. [95] proposed a new type of damper, which combines SMA elements with steel dampers based on a bending steel plate. Ma et al. [96] proposed a new SMA-based damper mainly consisting of pre-tensioned SMA wires and two pre-compressed springs; the damper shows both good energy dissipation capacity and re-centering capability. Fang et al. [97] proposed a new damper based on SMA ring spring as shown in Figure 13. Sui et al. [98] proposed a novel SMA-based damper making use of SMA wire, and the construction is designed so that the SMA wire is always stretched, whether the damper is in compression or tension. Qiu et al. [99] proposed an SMA-based anti-buckling damper by combining SMA bolts with a variable friction mechanism, as shown in Figure 14. It can be seen that whether the damper is in tension or compression, the SMA bolts is in tension, as shown in Figure 14b, thus effectively avoiding the problem of SMA bar buckling. Jia et al. [100] proposed an innovative double SMA damper system. In the proposed system, double SMA elements with different phase-transition temperatures are arranged in parallel. Fang et al. [101] proposed a shear damper based on an Fe-SMA. In comparative tests with a mild steel damper, it was found that the Fe-SMA dampers offer improved ductility and fatigue properties.

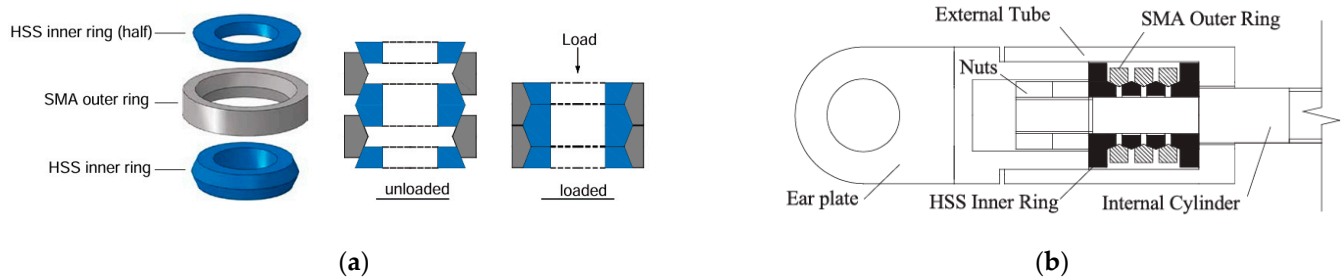


**Figure 13.** SMA ring spring damper [97]: (a) layout of SMA ring spring system; (b) layout of SMA damper. Reproduced with permission from [97], Elsevier, 2019.

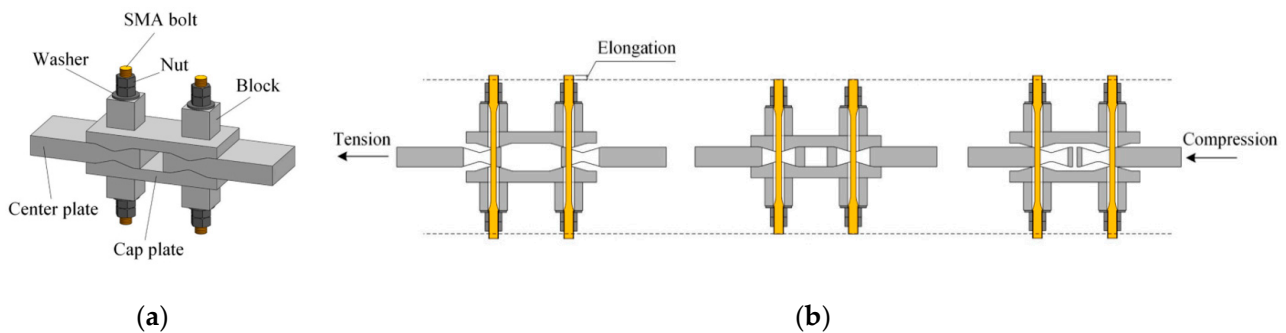


**Figure 14.** SMA slip friction damper [99]: (a) configuration; (b) sliding mechanism under axial loading reversals. Reproduced with permission from [99], Elsevier, 2022.

In addition, the SMA-based self-centering restrainers have also made great progress in research. Miller et al. [102] used SMA bars in BRB to reduce the residual deformation of the brace, as shown in Figure 15. It was found that the brace had good energy-dissipation and self-centering ability, and the self-centering ability was related to the SMA bars. Yang et al. [102] evaluated the performance of hybrid seismic bracing with a core consisting of SMA wires and energy-consuming struts, where the SMA wires were designed to be within a maximum strain of 6%. Numerical analysis shows that the frame structure with hybrid damping bracing can have similar energy-dissipation capacity as the BRB bracing system, and at the same time, it has better self-centering capacity. Shi et al. [103] proposed a brace based on SMA cables, and the cables are configured within a bracing system in a way that they are only subjected to tensile loads regardless of the loading direction of the bracing itself. Ozbulut et al. [104] proposed a method to optimize the design of SMA-based braces, and using this, the best SMA parameters can be obtained. In order to prevent buckling of SMA rods during compression, Cao et al. [105] proposed an anti-buckling system and designed long-stroke SMA restrainer (LSR). Study shows that the LSR can exhibit stable energy dissipation capabilities with excellent self-centering ability both under tension and compression loading. In addition, the numerical results show that the energy dissipation capacity, self-resetting capacity and limiting capacity of SMA rods in compression are much higher than those in tension. Fang et al. [106] proposed a self-centering brace that combines SMA bars and a friction system, as shown in Figure 16. As can be seen in Figure 17, the design concept of the brace is to provide stable energy dissipation through the friction system for the entire brace, and then utilize the SMA to provide the displacement-limiting capability and critical self-resetting capability for the brace.

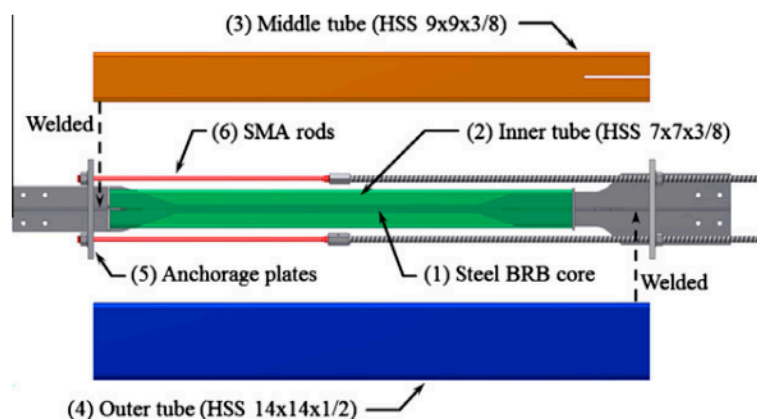


Figure 15. Self-centering buckling-restrained brace behavior, reproduced with permission from [102], Elsevier, 2012.

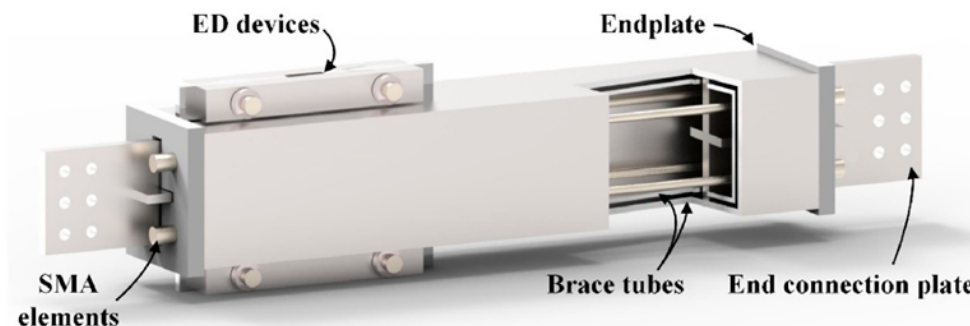


Figure 16. Configuration of the brace which is proposed by Fang, reproduced with permission from [106], Elsevier, 2012.

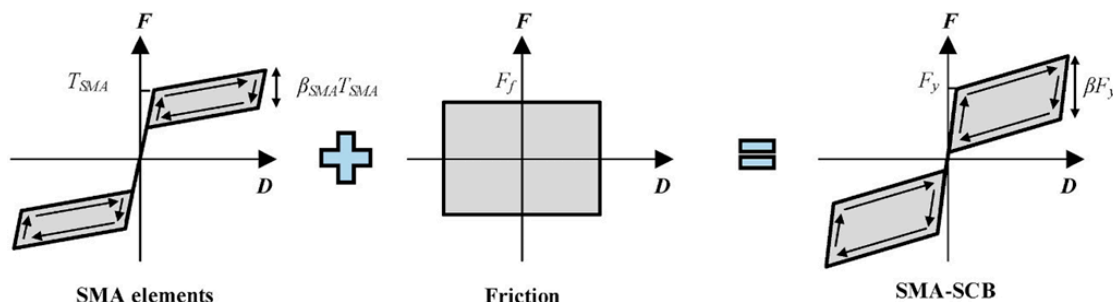


Figure 17. Idealized hysteretic behavior of the brace, reproduced with permission from [106], Elsevier, 2023.

### 6. Applications of SMA-Based Reinforcement in Steel Structures

The effectiveness of SMA-based components and technology in steel structure reinforcement needs to be demonstrated in its application. One notable example of SMA engineering applications is the practical reinforcement of cracked diaphragm cutouts on the Sutong Bridge. This application demonstrates the real-world effectiveness of SMAs in addressing structural issues and enhancing the durability and safety of critical infrastructure. This section discusses the application of SMAs in the field of steel structure reinforcement from three aspects: crack repair, seismic retrofit, and structural reinforcement.

#### 6.1. Crack Restoration

Fatigue cracks in steel structures can potentially lead to structural damage and failure. SMAs can be employed to repair these cracks by applying force in the affected area

to close the crack and maintain its stable state, preventing further crack propagation. Qiang et al. [107] proposed an Fe-SMA-plate-covering crack-stop holes method, and the repair process was shown in Figure 18.

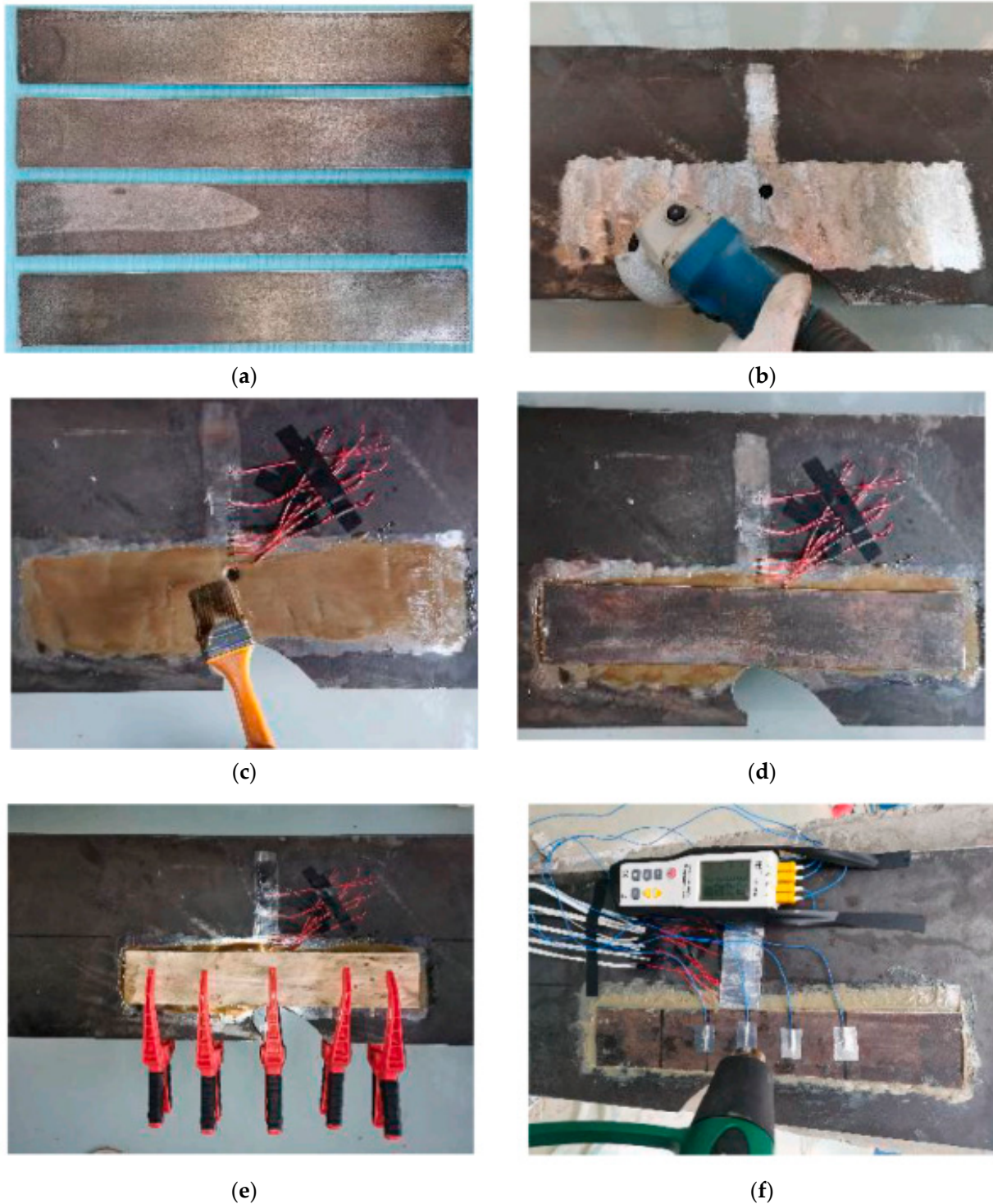


**Figure 18.** Repair process of the Fe-SMA strips covering crack-stop holes: (a) prepare pre-tensioned Fe-SMA strips; (b) polish and clean the steel strips; (c) apply structural adhesive; (d) bond Fe-SMA strips; (e) pressurized maintenance for five days; (f) activate Fe-SMA strips with a hot-air gun. Reproduced with permission from [107], Elsevier, 2023.

Pre-strained Fe-SMA patches were first applied to the reinforced area, and then, the Fe-SMA patches were thermally activated to repair the cracks using the shape memory effect of the SMA. The results show that the fatigue notch factor is reduced by 66.36% by bonding the Fe-SMA plate and can be further reduced by about 14% after activating the Fe-SMA. Izadi et al. [58] investigated the crack-repair effect of Fe-SMA strips using tests. The experimental results showed that Fe-SMA strips significantly increased the fatigue life of the specimens, and the stresses generated by the activated Fe-SMA strips could completely limit the development of fatigue cracks in the parent structure. In addition, Izadi et al. [59] used Fe-SMA strips to retrofit fatigue-cracked riveted connections in steel bridges. The results show that the crack development can be effectively inhibited and the load-bearing capacity can be increased by activating the SMA strips.

Zheng et al. [108] comparatively analyzed the effectiveness of SMA wire reinforcement, CFRP reinforcement, and SMA/CFRP reinforcement through experimental studies on the crack restoration of metallic structures, as shown in Figure 19. The results showed that the fatigue life of the members reinforced with an SMA wire and CFRP increased by 8 and 1.7 times, respectively, compared with that of the unreinforced members, while the fatigue life of the members reinforced with SMA/CFRP increased by 15–26 times. Kean et al. [109] investigated the factors affecting the reinforcement effect of SMA/CFRP composite patches through fatigue tests. The results showed that the factors affecting the reinforcing effect of steel include the amount of SMA, Young's modulus of CFRP, crack type, and crack width, and the reinforcing effect of the edge-cracked specimen was better than that of the center-cracked specimen. Qiang et al. [110] proposes two repair methods of the CFRP sheets and SMA/CFRP composite patches on the basis of crack-stop holes to repair cracks of the diaphragm cutouts. Fatigue tests showed that the fatigue notch factor of CFRP and SMA/CFRP patches decreased by 12.28% and 30.76%, respectively, compared to the placement of stopcrack holes only. Deng et al. [111] experimentally investigated the reinforcing effect of SMA/CFRP composite patches, and the results show that the SMA/CFRP composite patch can increase the fatigue life of the parent structure by about 8 times compared with the control specimen, which is much better than using SMA or CFRP reinforcement alone.

### 6.2. Bearing Capacity Reinforcement

The first practical engineering application of Fe-SMA strips in the reinforcement of a bridge structure was in the metallic girder of a historical roadway bridge in Petrov and Desnou, Czech Republic, where pre-strained Fe-SMA strips were reinforced to the steel girders, as shown in Figure 20. The results showed that Fe-SMA strips can effectively improve the force on the lower flange of the steel girder and increase the yield strength and ultimate bearing capacity of the steel girder [112]. Furthermore, Deng et al. [113] used SMA/CFRP composite sheets to improve the flexural stiffness of notched steel beams. The four-point bending test results showed that compared with the unreinforced beams, the ultimate load and flexural stiffness of the SMA/CFRP-composite-reinforced beams increased by 79.2% and 57.9%, respectively, basically equal to the sum of the effects of the SMA reinforcement alone and CFRP reinforcement alone. Hosseinejad et al. [114,115] increased the bearing capacity of steel beams by arranging pre-stressed SMA tendons outside their bodies. The analysis results show that the arrangement of SMA tendons increases the structural-load-carrying capacity more than the arrangement of steel tendons, and the pre-stressing is conveniently applied.

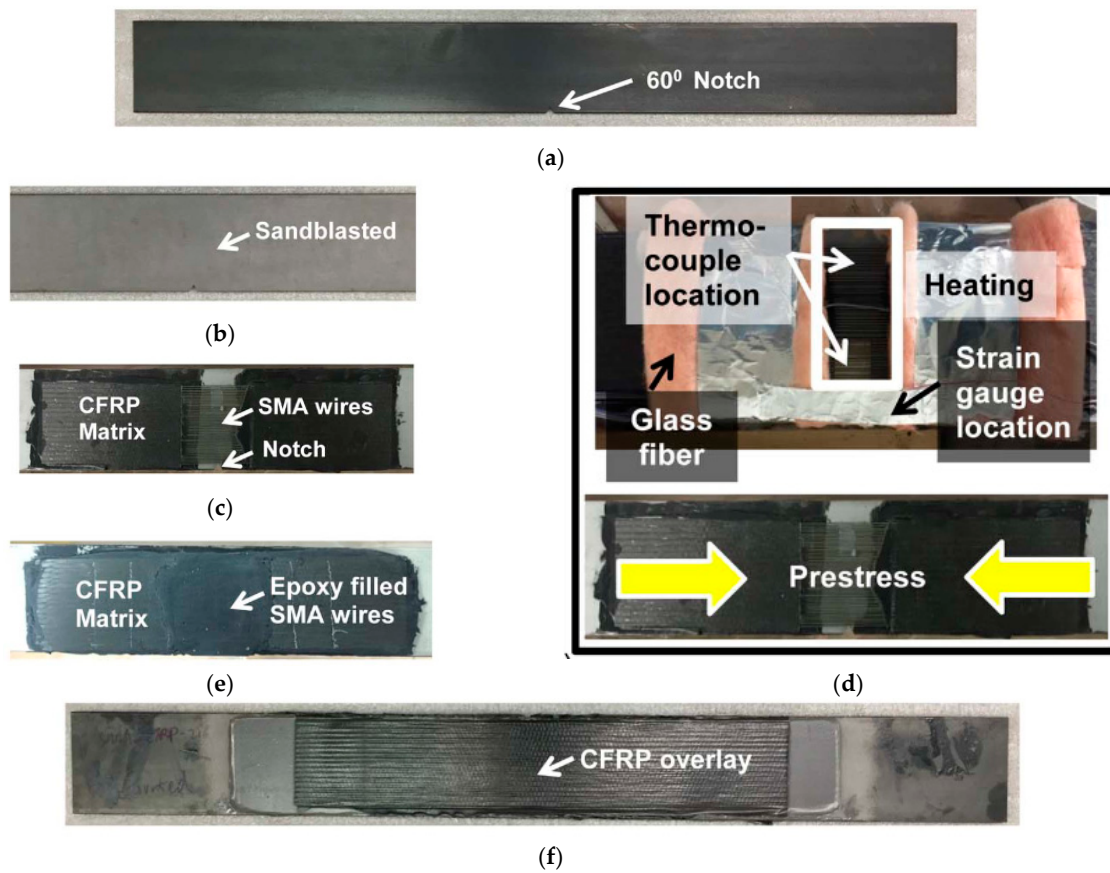


**Figure 19.** Process of strengthening the steel plate with an SMA/CFRP patch: (a) notched steel plate; (b) the plate surface after sand-blasting and cleaning; (c) SMA wires are placed; (d) the SMA wires were activated after the epoxy cured for 7 days; (e) the exposed SMA wires were covered with a structural epoxy paste after activation; (f) two layers of the HM carbon fiber were overlaid on top of the SMA wires. Reproduced with permission from [108], American society OF Civil Engineers, 1997.



**Figure 20.** Historic steel road bridge: (a) 3D view; (b) damage point 1; (c) damage point 2; (d) installation of the Fe-SMA strips. Reproduced with permission from [112], Elsevier, 2021.

### 6.3. Seismic Retrofitting

One of the important applications of SMAs is the seismic retrofit of steel structures. Researchers have investigated the use of SMAs as energy-dissipation and limiting devices in seismic systems.

Xing et al. [116] simulated the seismic response of a steel frame with SMA dampers, and the displacement and acceleration of the structure was reduced by at least 50%. Li et al. [117] proposed a double X-typed SMA (DX-SMA) damper, and it was installed in a frame-typed bridge pier, as shown in Figure 21. The results of the time–history analysis show that the installation of the DX-SMA increased the overall displacement-limiting capacity of the structure and reduced the residual displacement of the structure. Lv et al. [118] combined the SMA with TMD to develop a new damper, called SMAS-TMD, and the seismic performance of the frame equipped with the SMA-TMD was analyzed via shake table tests. The results show that combining SMA with TMD can effectively suppress the detuning phenomenon that often occurs in the classical optimal TMD. Qiu et al. [119] placed an SMA-based innovative self-centering damper on a steel frame, and then, the earthquake excitations were applied to the structures. Numerical results show that the displacement response of the structure equipped with SMA-based dampers is significantly reduced compared to the original structure.

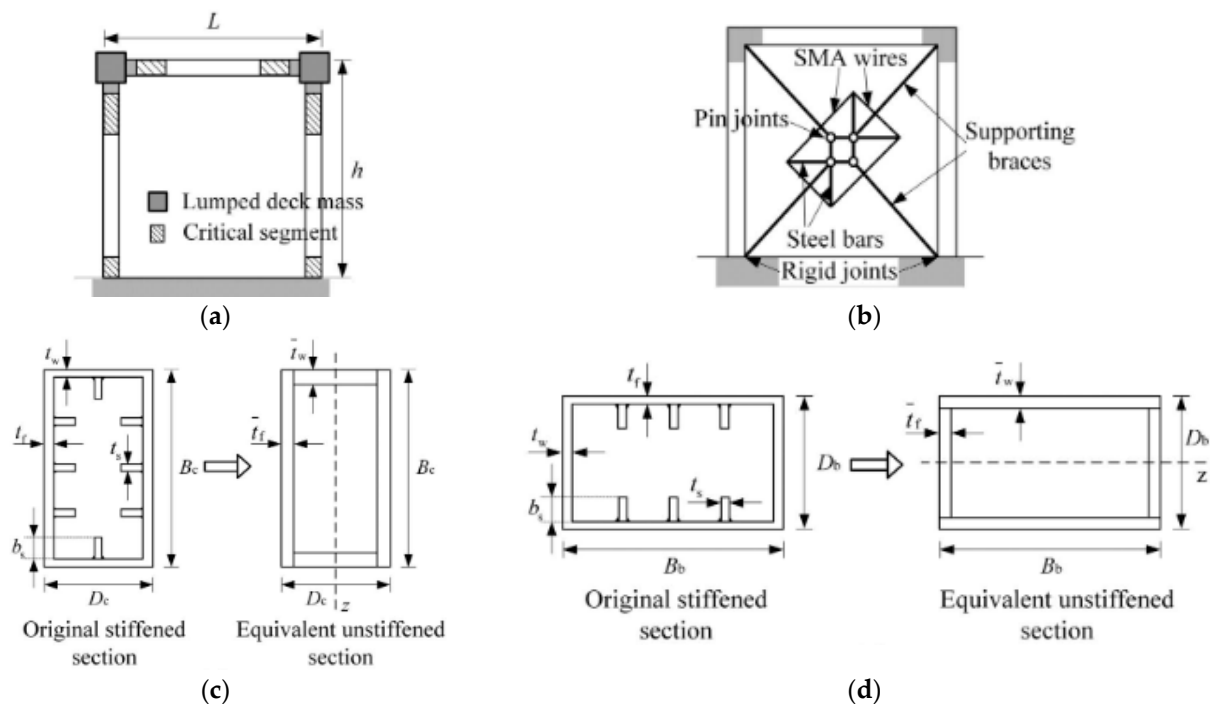


**Figure 21.** Model of bridge pier: (a) main frame; (b) bridge pier with DX-SMA damper; (c) column section; (d) beam section. Reproduced with permission from [117], American society OF Civil Engineers, 1988.

Asgarian et al. [120,121] compared and analyzed the seismic performance of steel frames equipped with SMA braces and BRB, where the SMA brace is arranged in a similar manner to the BRB, as shown in Figure 22. The result showed that SMA can improve the dynamic response of structures subjected to earthquake excitations, but the energy dissipation of structures with the BRB system was higher than that of structures with the SMA bracing system. Fahiminia et al. [122] used BRKB in two structures with different numbers of layers and added SMA to the core of BRKB. Subsequently, nonlinear time–history analysis of the two structures was carried out, and the results showed that adding SMA to the BRKBs can reduce the residual deformations of the frames by more than 50%. Vafaei et al. [123] studied the response of the SMA mega brace under seismic action. The

analysis results show that SMA braces exhibit better performance than BRB braces under near-field seismicity, but under far-field seismicity, SMA braces produce larger interlayer displacement angles. Qiu et al. [124] proposed a novel SMA brace, and then, the seismic performance of the frame with the SMA brace was assessed via shake table tests. The results show that the structure has good self-centering ability, and the SMA bracing can withstand multiple earthquakes without repair after the earthquake. In addition, Qiu et al. [125] also proposed a design method for the seismic retrofit of steel frames with SMA-based bracing, and numerical simulations were performed to validate the proposed design method. The results show that the overall seismic performance of the structure can be improved by 10–30% with the reasonable selection and arrangement of SMA-based bracing.

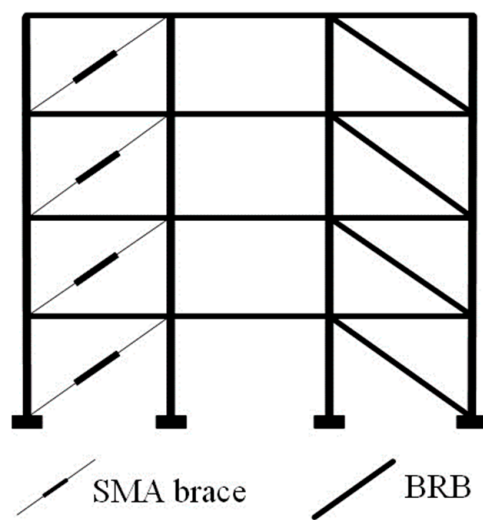


Figure 22. Arrangement of SMA brace.

## 7. Analysis and Discussion

- (1) At present, most of the research on SMAs is based on Nitinol-SMAs and has been more perfect, but the research on Fe-SMAs is still in the initial stage. Although Fe-SMAs are not as good as Nitinol-SMAs in terms of performance and the existence form, their relatively low price makes them have the potential to be widely used in practical engineering. Therefore, it is still necessary to take a step further into the basic mechanical behavior of Fe-SMAs and consider the factors affecting the mechanical properties of Fe-SMAs from the perspective of practical applications.
- (2) The design and development of SMA-based components are mainly focused on the seismic field, but there are relatively few in the field of structural reinforcement. In fact, SMAs have great potential for applications in the field of structural reinforcement, and their core competencies compared to traditional reinforcement methods include the following: (1) self-adaptability, SMAs possess shape memory properties, allowing them to adapt their shape based on external temperature or strain conditions. This means that SMAs can actively apply restoring forces when the structure is subjected to external loads or deformations, enhancing the structural stability and resistance; (2) lightweight, SMAs are relatively lightweight, so they can reinforce structures without adding excessive additional weight. This is particularly advantageous for situations where reducing loads is important, such as the maintenance and retrofitting of old or unstable structures; (3) minimal construction required, SMA reinforcement typically requires less construction work compared to traditional methods. This can reduce construction time and costs, as well as minimize disruption to the original structure; (4) excellent controllability, the properties of SMAs can be customized through alloy composition and heat treatment to meet specific engineering requirements. This allows for precise design and tuning based on the needs of a particular project; (5) high-temperature performance, SMAs typically exhibit good performance

at high temperatures, which is crucial for structures operating in high-temperature environments, such as industrial equipment or buildings in hot regions; (6) self-healing, SMAs have some degree of self-healing capability and can restore their original shape through external stimulation, reducing maintenance and repair costs. Therefore, there is still much room for research on and the development of SMA-based reinforcement components, both in terms of form and function.

- (3) Currently, the use of SMAs in steel structure reinforcement is not very common, and current research is still at the conceptualization stage; thus, there is a need to intensify research in this area. In addition to the above-mentioned research and development on material properties, SMA-based components, and technologies, there is a need to develop advanced construction techniques applicable to SMA reinforcement, such as SMA-activation methods and connection methods. On this basis, design methods for SMA-based structural steel reinforcement should be explored, and clear design guidelines and criteria should be established to ensure the correct application of SMAs in different situations.
- (4) Although SMA-based reinforcement can be used as a potential alternative to traditional reinforcement methods due to its unique characteristics, an assessment of its cost-effectiveness in practical applications is indispensable. Currently, there are fewer cost-effectiveness analyses of SMA-based reinforcement methods, and they are only considered in terms of static indicators, such as the material cost, construction cost, and labor [39], ignoring the advantages of the material properties of SMAs under long-term service. Therefore, to make an accurate comparison between the cost-effectiveness of SMAs and traditional methods, a comprehensive life-cycle cost analysis should be conducted. In addition to the static indicators mentioned earlier, the following factors should be considered in the analysis: (1) long-term performance and maintenance costs, when properly designed and implemented, SMAs provide long-term benefits by reducing the need for frequent maintenance and repairs. They are able to recover from deformations caused by external factors, resulting in cost savings over the entire life cycle of the structure; (2) energy and environmental impact, although the production of SMAs might have a higher energy cost compared to traditional reinforcement materials, the potential long-term benefits in terms of reduced maintenance and repair could lead to lower energy consumption and a smaller environmental footprint; (3) structural performance and safety, SMAs offer unique advantages in terms of improving the structural performance and safety of steel structures, especially in high-stress environments. Their ability to absorb energy and recover from deformations can contribute to improved resilience and reduced risks of structural failure.
- (5) In recent years, a large number of SMA-based anti-flexural braces have been proposed and have demonstrated excellent self-centering, displacement-limiting, and energy-dissipation capabilities. The anti-flexing principle is to avoid pressure on SMA bars, which is effective but wastes the excellent compression properties of SMAs. Therefore, it is necessary to investigate anti-flexural bracing that preserves the compressive properties of SMAs to maximize the mechanical properties of SMAs, such as the LSR proposed by Cao et al. [104].
- (6) Research on and the development of SMAs continue to evolve, with a focus on expanding their applications in civil engineering. Several potential future directions and emerging trends could impact the use of SMAs in structural reinforcement: (1) improved material performance, develop novel SMA compositions and refine the manufacturing processes to create more robust and cost-effective materials for civil engineering applications; (2) integration of smart technologies, the integration of SMAs with smart sensing and monitoring technologies is an emerging trend. This integration could enable the early detection of potential structural failures and improve maintenance strategies; (3) advancements in 3D printing techniques, 3D printing technology offers new possibilities for the fabrication of complex SMA-based

structural components with intricate geometries. Research efforts are focusing on developing innovative 3D printing techniques that can produce customized SMA elements, leading to more efficient and precise structural reinforcement solutions; (4) nanostructured SMAs, the development of nanostructured SMAs with excellent mechanical properties and higher performance characteristics for better resistance to wear, corrosion, and fatigue.

- (7) Temperature has a very significant effect on the fatigue properties of SMAs, and annealing changes the transition temperature of SMAs. There is little information available on whether the change in the transition temperature due to annealing improves the fatigue properties of SMAs at different temperatures. This knowledge gap needs to be bridged in future studies.

## 8. Conclusions

- (1) The study of the mechanical behavior of Fe-SMAs under different environmental conditions needs to be strengthened, and the influence of the loading history on the shape memory effect is not well understood.
- (2) The research on SMA-based reinforcement components and techniques needs to be deepened, especially for Fe-SMA-based components.
- (3) Previous studies have only focused on the fatigue performance of SMA reinforcement and have not analyzed the improvement of the overall seismic performance of the structure after SMA reinforcement. Due to the characteristics of SMAs, this aspect of research should also be emphasized.
- (4) A rational design method is the basis for engineering applications. Scholars have verified the feasibility of applying SMAs to steel structure reinforcement, but no comprehensive SMA-based design method has been proposed for steel structure reinforcement.
- (5) Little attention has been paid to the fatigue performance of SMAs, and most studies have not considered the effects of environmental factors. Therefore, the fatigue performance of SMAs under the coupling of various environmental factors should be studied more thoroughly.
- (6) Annealing has a very important effect on the mechanical properties of SMAs, and a suitable annealing program can reduce the residual deformation of SMAs by more than 50%. However, most of the current research in this field has been performed from a superelasticity point of view to find the optimal annealing solution for a specific SMA part. The effect of annealing on its law should be studied in depth from several angles, such as the fatigue life of SMAs.
- (7) The cost-effectiveness of SMA reinforcement techniques cannot be analyzed only from a static point of view, such as material costs and construction costs. They should also be analyzed in terms of life-cycle costs, taking into account the long-term performance, environmental impact, and structural performance and safety.

**Author Contributions:** Conceptualization, Y.H.; methodology, Y.H. and C.S.; writing—original draft preparation, Y.H.; writing—review and editing, Y.H. and C.S.; project administration, Y.H.; funding acquisition, Y.H. All authors have read and agreed to the published version of the manuscript.

**Funding:** This research was funded by the Natural Science Foundation of Guangdong Province (2022A1515012589), the “111” Project (No. D21021), and the Technology Planning Project of Guangzhou City (No. 202201020143).

**Data Availability Statement:** The data presented in this study are available on request from the corresponding author.

**Acknowledgments:** The authors would like to thank all partners of the Research Center of Wind Engineering and Engineering Vibration, Guangzhou University, for their contribution to this research.

**Conflicts of Interest:** The authors declare no conflict of interest.

## References

1. Kirk, R.S.; Mallett, W.J. *Highway Bridge Conditions: Issues for Congress*. Library of Congress; Congressional Research Service: Washington, DC, USA, 2014.
2. Woo, S.K.; Nam, J.W.; Kim, J.H.J.; Han, S.H.; Byun, K.J. Suggestion of flexural capacity evaluation and prediction of prestressed CFRP strengthened design. *Eng. Struct.* **2008**, *30*, 3751–3763. [[CrossRef](#)]
3. Kamruzzaman, M.; Jumaat, M.Z.; Sulong, N.H.R.; Islam, A. A Review on Strengthening Steel Beams Using FRP under Fatigue. *Sci. World J.* **2014**. [[CrossRef](#)] [[PubMed](#)]
4. Dogar, A.U.R.; Rehman, H.; Tafsirojaman, T.; Iqbal, N. Experimental investigations on inelastic behaviour and modified Gerber joint for double-span steel trapezoidal sheeting. *Structures* **2020**, *24*, 514–525. [[CrossRef](#)]
5. Olofsson, I.; Elfgren, L.; Bell, B.; Paulsson, B.; Niederleithinger, E.; Jensen, J.S.; Feltrin, G.; Taljsten, B.; Cremona, C.; Kiviluoma, R.; et al. Assessment of European railway bridges for future traffic demands and longer lives—EC project “Sustainable Bridges”. *Struct. Infrastruct. Eng.* **2005**, *1*, 93–100. [[CrossRef](#)]
6. Wang, W.; Chan, T.-M.; Zhang, Y.; Engineering, C. Special issue on resilience in steel structures. *Front. Struct.* **2016**, *10*, 237–238. [[CrossRef](#)]
7. Liu, B.F.; Wang, Q.F.; Hu, S.L.; Zhang, W.; Du, C.Z. On thermomechanical behaviors of the functional graded shape memory alloy composite for jet engine chevron. *J. Intell. Mater. Syst. Struct.* **2018**, *29*, 2986–3005. [[CrossRef](#)]
8. Zhou, J.W.; Hou, J.Y.; Shi, Y.T. Shape Memory Alloy Materials and Exercise-induced Bone Injury. In Proceedings of the International Conference on Mechanical Engineering, Civil Engineering and Material Engineering (MECEM 2013), Hefei, China, 27–28 October 2013; pp. 257–262.
9. Fallon, P.D.; Gerratt, A.P.; Kierstead, B.P.; White, R.D. Shape Memory Alloy and Elastomer Composite MEMS Actuators. In Proceedings of the Nanotechnology Conference and Trade Show (Nanotech 2008), Boston, MA, USA, 1–5 June 2008; pp. 470–473.
10. Zhou, X.L.; Yuan, Q.J.; Chen, L.; Chen, J.; Deng, T.X.; Hu, Y.Q.; Li, A. Determination of the Design Parameters of SMA Cables for Self-Centering Frame Structures. *Buildings* **2023**, *13*, 1019. [[CrossRef](#)]
11. Hong, K.N.; Yeon, Y.M.; Ji, S.W.; Lee, S. Flexural Behavior of RC Beams Using Fe-Based Shape Memory Alloy Rebars as Tensile Reinforcement. *Buildings* **2022**, *12*, 190. [[CrossRef](#)]
12. Yang, T.; Liu, S.L.; Xiong, S.Y.; Liu, Y.; Liu, B.; Li, B.B. Simulation Analysis of the Small Wild Goose Pagoda Structure Using a Shape Memory Alloy-Suspension Pendulum Damping System (SMA-SPDS). *Buildings* **2022**, *12*, 686. [[CrossRef](#)]
13. Foraboschi, P. Predictive formulation for the ultimate combinations of axial force and bending moment attainable by steel members. *Int. J. Steel Struct.* **2020**, *20*, 705–724. [[CrossRef](#)]
14. Foraboschi, P. Lateral load-carrying capacity of steel columns with fixed-roller end supports. *J. Build. Eng.* **2019**, *26*, 100879. [[CrossRef](#)]
15. Zareie, S.; Issa, A.S.; Seethaler, R.J.; Zabihollah, A. Recent advances in the applications of shape memory alloys in civil infrastructures: A review. *Structures* **2020**, *27*, 1535–1550. [[CrossRef](#)]
16. Fang, C.; Zheng, Y.; Chen, J.B.; Yam, M.C.H.; Wang, W. Superelastic NiTi SMA cables: Thermal-mechanical behavior, hysteretic modelling and seismic application. *Eng. Struct.* **2019**, *183*, 533–549. [[CrossRef](#)]
17. Ghafoori, E.; Wang, B.; Andrawes, B. Shape memory alloys for structural engineering: An editorial overview of research and future potentials. *Eng. Struct.* **2022**, *273*, 115138. [[CrossRef](#)]
18. Alam, M.S.; Youssef, M.A.; Nehdi, M. Analytical prediction of the seismic behaviour of superelastic shape memory alloy reinforced concrete elements. *Eng. Struct.* **2008**, *30*, 3399–3411. [[CrossRef](#)]
19. Fang, C.; Zhou, X.Y.; Osofero, A.I.; Shu, Z.; Corradi, M. Superelastic SMA Belleville washers for seismic resisting applications: Experimental study and modelling strategy. *Smart Mater. Struct.* **2016**, *25*, 105013. [[CrossRef](#)]
20. Park, J.; Choi, E.; Park, K.; Kim, H.T. Comparing the cyclic behavior of concrete cylinders confined by shape memory alloy wire or steel jackets. *Smart Mater. Struct.* **2011**, *20*, 094008. [[CrossRef](#)]
21. Araki, Y.; Endo, T.; Omori, T.; Sutou, Y.; Koetaka, Y.; Kainuma, R.; Ishida, K. Potential of superelastic Cu-Al-Mn alloy bars for seismic applications. *Earthq. Eng. Struct. Dyn.* **2011**, *40*, 107–115. [[CrossRef](#)]
22. Zhang, Y.F.; Hu, X.B.; Zhu, S.Y. Seismic performance of benchmark base-isolated bridges with superelastic Cu-Al-Be restraining damping device. *Struct. Control Health Monit.* **2009**, *16*, 668–685. [[CrossRef](#)]
23. Rojob, H.; El-Hacha, R. Self-Prestressing Using Iron-Based Shape Memory Alloy for Flexural Strengthening of Reinforced Concrete Beams. *ACI Struct. J.* **2017**, *114*, 523–532. [[CrossRef](#)]
24. El Naggar, A.; Youssef, M.A. Shape memory alloy heat activation: State of the art review. *Aims Mater. Sci.* **2020**, *7*, 836–858. [[CrossRef](#)]
25. Zhang, Z.X.; Zhang, J.; Wu, H.L.; Ji, Y.Z.; Kumar, D.D. Iron-Based Shape Memory Alloys in Construction: Research, Applications and Opportunities. *Materials* **2022**, *15*, 1723. [[CrossRef](#)]
26. Yang, Z.; Li, J.K.; Zhong, Y.L.; Qi, X.L. Mechanical Properties of SMA/PVA-ECC under Uniaxial Tensile Loading. *Buildings* **2023**, *13*, 2116. [[CrossRef](#)]
27. Billah, A.M.; Rahman, J.; Zhang, Q. Shape memory alloys (SMAs) for resilient bridges: A state-of-the-art review. *Structures* **2022**, *37*, 514–527. [[CrossRef](#)]
28. Frick, C.P.; Ortega, A.M.; Tyber, J.; Maksound, A.E.M.; Maier, H.J.; Liu, Y.N.; Gall, K. Thermal processing of polycrystalline NiTi shape memory alloys. *Mater. Sci. Eng. A-Struct. Mater. Prop. Microstruct. Process.* **2005**, *405*, 34–49. [[CrossRef](#)]

29. Mahtabi, M.J.; Shamsaei, N.; Rutherford, B. Mean strain effects on the fatigue behavior of superelastic Nitinol alloys: An experimental investigation. In Proceedings of the 6th International Conference on Fatigue Design (Fatigue Design), Senlis, France, 18–19 November 2015; pp. 646–654.
30. Saikrishna, C.N.; Ramaiah, K.V.; Paul, D.; Bhaumik, S.K. Enhancement in fatigue life of NiTi shape memory alloy thermal actuator wire. *Acta Mater.* **2016**, *102*, 385–396. [[CrossRef](#)]
31. Miyazaki, S.; Mizukoshi, K.; Ueki, T.; Sakuma, T.; Liu, Y.N. Fatigue life of Ti-50 at.% Ni and Ti-40Ni-10Cu (at.%) shape memory alloy wires. *Mater. Sci. Eng. A-Struct. Mater. Prop. Microstruct. Process.* **1999**, *273*, 658–663. [[CrossRef](#)]
32. Koster, M.; Lee, W.; Schwarzenberger, M.; Leinenbach, C. Cyclic deformation and structural fatigue behavior of an Fe-Mn-Si shape memory alloy. *Mater. Sci. Eng. A* **2015**, *637*, 29–39. [[CrossRef](#)]
33. Li, L.; Zhao, X.X.; Cheng, J.W. Research on Fatigue Performance of Shape-Memory Alloy Bars under Low Cyclic Loading. *Buildings* **2023**, *13*, 1553. [[CrossRef](#)]
34. Yang, Z.; Deng, T.Y.; Fu, Q.S. The Effect of Fiber End on the Bonding Mechanical Properties between SMA Fibers and ECC Matrix. *Buildings* **2023**, *13*, 2027. [[CrossRef](#)]
35. Lin, C.K.; Wang, Z.Q.; Yang, X.; Zhou, H.J. Experimental Study on Temperature Effects on NiTi Shape Memory Alloys under Fatigue Loading. *Materials* **2020**, *13*, 573. [[CrossRef](#)] [[PubMed](#)]
36. Gu, X.L.; Chen, Z.Y.; Yu, Q.Q.; Ghafoori, E. Stress recovery behavior of an Fe-Mn-Si shape memory alloy. *Eng. Struct.* **2021**, *243*, 112710. [[CrossRef](#)]
37. Cladera, A.; Weber, B.; Leinenbach, C.; Czaderski, C.; Shahverdi, M.; Motavalli, M. Iron-based shape memory alloys for civil engineering structures: An overview. *Constr. Build. Mater.* **2014**, *63*, 281–293. [[CrossRef](#)]
38. Yeon, Y.M.; Nam, H.K.; Lee, J.; Sangwon, J. Evaluation of Corrosion Behavior for Fe-based Shape Memory Alloy. *J. Korean Soc. Adv. Compos. Struct.* **2021**, *12*, 50–56. [[CrossRef](#)]
39. Hosseini, A.; Michels, J.; Izadi, M.; Ghafoori, E. A comparative study between Fe-SMA and CFRP reinforcements for prestressed strengthening of metallic structures. *Constr. Build. Mater.* **2019**, *226*, 976–992. [[CrossRef](#)]
40. Wang, S.Z.; Li, L.Z.; Su, Q.T.; Jiang, X.; Ghafoori, E. Strengthening of steel beams with adhesively bonded memory-steel strips. *Thin-Walled Struct.* **2023**, *189*, 110901. [[CrossRef](#)]
41. Li, L.; Wang, S.; Chatzi, E.; Motavalli, M.; Ghafoori, E. Prediction of prestress level in steel structures strengthened by bonded Fe-SMA strips. *ce/papers* **2023**, *6*, 364–368. [[CrossRef](#)]
42. Hong, K.; Lee, S.; Han, S.; Yeon, Y. Evaluation of Fe-Based Shape Memory Alloy (Fe-SMA) as Strengthening Material for Reinforced Concrete Structures. *Appl. Sci.* **2018**, *8*, 730. [[CrossRef](#)]
43. Ghafoori, E.; Hosseini, E.; Leinenbach, C.; Michels, J.; Motavalli, M. Fatigue behavior of a Fe-Mn-Si shape memory alloy used for prestressed strengthening. *Mater. Des.* **2017**, *133*, 349–362. [[CrossRef](#)]
44. Marinopoulou, E.; Katalalos, K. Thermomechanical Fatigue Testing on Fe-Mn-Si Shape Memory Alloys in Prestress Conditions. *Materials* **2023**, *16*, 237. [[CrossRef](#)]
45. Hosseini, E.; Ghafoori, E.; Leinenbach, C.; Motavalli, M.; Holdsworth, S.R. Stress recovery and cyclic behaviour of an Fe-Mn-Si shape memory alloy after multiple thermal activation. *Smart Mater. Struct.* **2018**, *27*, 025009. [[CrossRef](#)]
46. Izadi, M.; Hosseini, A.; Michels, J.; Motavalli, M.; Ghafoori, E. Thermally activated iron-based shape memory alloy for strengthening metallic girders. *Thin-Walled Struct.* **2019**, *141*, 389–401. [[CrossRef](#)]
47. Dong, Z.Z.; Klotz, U.E.; Leinenbach, C.; Bergamini, A.; Czaderski, C.; Motavalli, M. A Novel Fe-Mn-Si Shape Memory Alloy With Improved Shape Recovery Properties by VC Precipitation. *Adv. Eng. Mater.* **2009**, *11*, 40–44. [[CrossRef](#)]
48. Leinenbach, C.; Kramer, H.; Bernhard, C.; Eifler, D. Thermo-Mechanical Properties of an Fe-Mn-Si-Cr-Ni-VC Shape Memory Alloy with Low Transformation Temperature. *Adv. Eng. Mater.* **2012**, *14*, 62–67. [[CrossRef](#)]
49. Czaderski, C.; Shahverdi, M.; Bronnimann, R.; Leinenbach, C.; Motavalli, M. Feasibility of iron-based shape memory alloy strips for prestressed strengthening of concrete structures. *Constr. Build. Mater.* **2014**, *56*, 94–105. [[CrossRef](#)]
50. Lee, W.J.; Weber, B.; Leinenbach, C. Recovery stress formation in a restrained Fe-Mn-Si-based shape memory alloy used for prestressing or mechanical joining. *Constr. Build. Mater.* **2015**, *95*, 600–610. [[CrossRef](#)]
51. Shahverdi, M.; Czaderski, C.; Motavalli, M. Iron-based shape memory alloys for prestressed near-surface mounted strengthening of reinforced concrete beams. *Constr. Build. Mater.* **2016**, *112*, 28–38. [[CrossRef](#)]
52. Izadi, M.R.; Ghafoori, E.; Shahverdi, M.; Motavalli, M.; Maalek, S. Development-of an iron-based shape memory alloy (Fe-SMA) strengthening system for steel plates. *Eng. Struct.* **2018**, *174*, 433–446. [[CrossRef](#)]
53. Michels, J.; Shahverdi, M.; Czaderski, C. Flexural strengthening of structural concrete with iron-based shape memory alloy strips. *Struct. Concr.* **2018**, *19*, 876–891. [[CrossRef](#)]
54. Dong, Z.Z.; Sawaguchi, T.; Kajiwara, S.; Kikuchi, T.; Kim, S.H.; Lee, G.C. Microstructure change and shape memory characteristics in welded Fe-28Mn-6Si-5Cr-0.53Nb-0.06C alloy. *Mater. Sci. Eng. A-Struct. Mater. Prop. Microstruct. Process.* **2006**, *438*, 800–803. [[CrossRef](#)]
55. Soroushian, P.; Ostowari, K.; Nossoni, A.; Chowdhury, H. Repair and Strengthening of Concrete Structures Through Application of Corrective Posttensioning Forces with Shape Memory Alloys. *Transp. Res. Rec.* **2001**, *1770*, 20–26. [[CrossRef](#)]
56. Hong, K.; Lee, S.; Yeon, Y.; Jung, K. Flexural Response of Reinforced Concrete Beams Strengthened with Near-Surface-Mounted Fe-Based Shape-Memory Alloy Strips. *Int. J. Concr. Struct. Mater.* **2018**, *12*, 45. [[CrossRef](#)]

57. El-Hacha, R.; Rojob, H. Flexural strengthening of large-scale reinforced concrete beams using near-surface -mounted self-prestressed iron-based shape-memory alloy strips. *PCI J.* **2018**, *63*, 55–65. [[CrossRef](#)]
58. Izadi, M.R.; Ghafoori, E.; Motavalli, M.; Maalek, S. Iron-based shape memory alloy for the fatigue strengthening of cracked steel plates: Effects of re-activations and loading frequencies. *Eng. Struct.* **2018**, *176*, 953–967. [[CrossRef](#)]
59. Izadi, M.; Motavalli, M.; Ghafoori, E. Iron-based shape memory alloy (Fe-SMA) for fatigue strengthening of cracked steel bridge connections. *Constr. Build. Mater.* **2019**, *227*, 116800. [[CrossRef](#)]
60. Qiang, X.; Duan, X.; Jiang, X.; Lu, Q.; Zhou, G.J.E.S. Experimental study on mechanical properties of bolted joints between Fe-SMA and steel plates. *Eng. Struct.* **2023**, *297*, 116980. [[CrossRef](#)]
61. Qiang, X.H.; Wu, Y.P.; Wang, Y.H.; Jiang, X. Research Progress and Applications of Fe-Mn-Si-Based Shape Memory Alloys on Reinforcing Steel and Concrete Brdiges. *Appl. Sci.* **2023**, *13*, 3404. [[CrossRef](#)]
62. Fritsch, E.; Izadi, M.; Ghafoori, E. Development of nail-anchor strengthening system with iron-based shape memory alloy (Fe-SMA) strips. *Constr. Build. Mater.* **2019**, *229*, 117042. [[CrossRef](#)]
63. Wang, W.D.; Li, L.Z.; Hosseini, A.; Ghafoori, E. Novel fatigue strengthening solution for metallic structures using adhesively bonded Fe-SMA strips: A proof of concept study. *Int. J. Fatigue* **2021**, *148*, 106237. [[CrossRef](#)]
64. Li, L.Z.; Chatzi, E.; Ghafoori, E. Debonding model for nonlinear Fe-SMA strips bonded with nonlinear adhesives. *Eng. Fract. Mech.* **2023**, *282*, 109201. [[CrossRef](#)]
65. Li, L.Z.; Wang, W.D.; Chatzi, E.; Ghafoori, E. Experimental investigation on debonding behavior of Fe-SMA-to-steel joints. *Constr. Build. Mater.* **2023**, *364*, 129857. [[CrossRef](#)]
66. Choi, E.; Ostadrahimi, A.; Kim, W.J.; Seo, J. Prestressing effect of embedded Fe-based SMA wire on the flexural behavior of mortar beams. *Eng. Struct.* **2021**, *227*, 111472. [[CrossRef](#)]
67. Shahverdi, M.; Czaderski, C.; Annen, P.; Motavalli, M. Strengthening of RC beams by iron-based shape memory alloy bars embedded in a shotcrete layer. *Eng. Struct.* **2016**, *117*, 263–273. [[CrossRef](#)]
68. Wang, C.P.; Wen, Y.H.; Peng, H.B.; Xu, D.Q.; Li, N. Factors affecting recovery stress in Fe-Mn-Si-Cr-Ni-C shape memory alloys. *Mater. Sci. Eng. A-Struct. Mater. Prop. Microstruct. Process.* **2011**, *528*, 1125–1130. [[CrossRef](#)]
69. Wang, Z.Y.; Wang, Q.Y.; Li, L.H.; Zhang, N. Fatigue behaviour of CFRP strengthened open-hole steel plates. *Thin-Walled Struct.* **2017**, *115*, 176–187. [[CrossRef](#)]
70. Aljabar, N.J.; Zhao, X.L.; Al-Mahaidi, R.; Ghafoori, E.; Motavalli, M.; Powers, N. Effect of crack orientation on fatigue behavior of CFRP-strengthened steel plates. *Compos. Struct.* **2016**, *152*, 295–305. [[CrossRef](#)]
71. Chen, T.; Gu, X.L.; Qi, M.; Yu, Q.Q. Experimental Study on Fatigue Behavior of Cracked Rectangular Hollow-Section Steel Beams Repaired with Prestressed CFRP Plates. *J. Compos. Constr.* **2018**, *22*, 04018034. [[CrossRef](#)]
72. Colombi, P.; Fava, G.; Sonzogno, L. Fatigue crack growth in CFRP-strengthened steel plates. *Compos. Part B-Eng.* **2015**, *72*, 87–96. [[CrossRef](#)]
73. Colombi, P.; Fava, G. Experimental study on the fatigue behaviour of cracked steel beams repaired with CFRP plates. *Eng. Fract. Mech.* **2015**, *145*, 128–142. [[CrossRef](#)]
74. Xu, Y.; Otsuka, K.; Toyama, N.; Yoshida, H.; Nagai, H.; Oishi, R.; Kikushima, Y.; Yuse, K.; Akimune, Y.; Kishi, T. Fabrication technique of SMA/CFRP smart composites. In Proceedings of the Conference on Transducing Materials and Devices, Brugge, Belgium, 30 October–1 November 2002; pp. 35–46.
75. Li, L.Z.; Chen, T.; Gu, X.L.; Ghafoori, E. Heat Activated SMA-CFRP Composites for Fatigue Strengthening of Cracked Steel Plates. *J. Compos. Constr.* **2020**, *24*, 04020060. [[CrossRef](#)]
76. El-Tahan, M.; Dawood, M.; Song, G. Development of a self-stressing NiTiNb shape memory alloy (SMA)/fiber reinforced polymer (FRP) patch. *Smart Mater. Struct.* **2015**, *24*, 065035. [[CrossRef](#)]
77. Xue, Y.J.; Cai, D.C.; Wang, W.W.; Tian, J.; Zhen, J.S.; Li, B.C. Prestress loss and flexural behavior of precracked RC beams strengthened with FRP/SMA composites. *Compos. Struct.* **2023**, *321*, 117319. [[CrossRef](#)]
78. Xue, Y.J.; Wang, W.W.; Tan, X.; Hui, Y.X.; Tian, J.; Zhu, Z.F. Mechanical behavior and recoverable properties of CFRP shape memory alloy composite under different prestrains. *Constr. Build. Mater.* **2022**, *333*, 127186. [[CrossRef](#)]
79. Abdy, A.I.; Hashemi, M.J.; Al-Mahaidi, R. Fatigue life improvement of steel structures using self-prestressing CFRP/SMA hybrid composite patches. *Eng. Struct.* **2018**, *174*, 358–372. [[CrossRef](#)]
80. Jang, B.K.; Xu, Y.; Oishi, R.; Nagai, H.; Yoshida, H.; Akimune, Y.; Otsuka, K.; Kishi, T. Thermomechanical characterization and development of SMA embedded CFRP composites with self-damage control. In Proceedings of the Smart Structures and Materials 2002 Conference, San Diego, CA, USA, 18–21 March 2002; pp. 182–190.
81. Xue, Y.J.; Wang, W.W.; Wu, Z.H.; Hu, S.W.; Tian, J. Experimental study on flexural behavior of RC beams strengthened with FRP/SMA composites. *Eng. Struct.* **2023**, *289*, 116288. [[CrossRef](#)]
82. Xu, Y.; Otsuka, K.; Toyama, N.; Yoshida, H.; Jang, B.K.; Nagai, H.; Oishi, R.; Kishi, T. Fabrication of TiNi/CFRP smart composite using cold drawn TiNi wires. In Proceedings of the Smart Structures and Materials 2002 Conference, San Diego, CA, USA, 18–21 March 2002; pp. 564–574.
83. Xue, Y.J.; Wang, W.W.; Tian, J.; Wu, Z.H. Experimental study and analysis of RC beams shear strengthened with FRP/SMA composites. *Structures* **2023**, *55*, 1936–1948. [[CrossRef](#)]
84. Zheng, B.T.; El-Tahan, M.; Dawood, M. Shape memory alloy-carbon fiber reinforced polymer system for strengthening fatigue-sensitive metallic structures. *Eng. Struct.* **2018**, *171*, 190–201. [[CrossRef](#)]

85. El-Tahan, M.; Dawood, M. Bond behavior of NiTiNb SMA wires embedded in CFRP composites. *Polym. Compos.* **2018**, *39*, 3780–3791. [[CrossRef](#)]
86. Gu, X.J.; Su, X.Z.; Wang, J.; Xu, Y.J.; Zhu, J.H.; Zhang, W.H. Improvement of impact resistance of plain-woven composite by embedding superelastic shape memory alloy wires. *Front. Mech. Eng.* **2020**, *15*, 547–557. [[CrossRef](#)]
87. Yang, S.Y.; Goo, B.C.; Kim, H.J. Mechanical behavior of shape memory alloy composites. In *Advances in Fracture and Strength, Pts 1–4*; Kim, Y.J., Bae, H.D., Kim, Y.J., Eds.; Trans Tech Publications: Stafa, Switzerland, 2005; Volume 297–300, pp. 1551–1555.
88. El-Tahan, M.; Dawood, M. Fatigue behavior of a thermally-activated NiTiNb SMA-FRP patch. *Smart Mater. Struct.* **2016**, *25*, 015030. [[CrossRef](#)]
89. Deng, J.; Fei, Z.Y.; Li, J.H.; Li, H. Fatigue behaviour of notched steel beams strengthened by a self-prestressing SMA/CFRP composite. *Eng. Struct.* **2023**, *274*, 115077. [[CrossRef](#)]
90. Russian, O.; Belarbi, A.; Dawood, M. Effect of surface preparation technique on fatigue performance of steel structures repaired with self-stressing SMA/CFRP patch. *Compos. Struct.* **2022**, *280*, 114968. [[CrossRef](#)]
91. Fang, C.; Liang, D.; Zheng, Y.; Lu, S.Y. Seismic performance of bridges with novel SMA cable-restrained high damping rubber bearings against near-fault ground motions. *Earthq. Eng. Struct. Dyn.* **2022**, *51*, 44–65. [[CrossRef](#)]
92. Farhangi, V.; Jahangir, H.; Eidgahee, D.R.; Karimipour, A.; Javan, S.A.N.; Hasani, H.; Fasihhour, N.; Karakouzian, M.J.A.S. Behaviour investigation of SMA-equipped bar hysteretic dampers using machine learning techniques. *Appl. Sci.* **2021**, *11*, 10057. [[CrossRef](#)]
93. Liu, A.R.; Yu, Q.C.; Zhang, J.P.; Xie, S.F.; Guo, Y.Z. Study on Vibration Control of Long Cable with Shape Memory Alloy Damper. *Adv. Sci. Lett.* **2011**, *4*, 3023–3026. [[CrossRef](#)]
94. Han, Y.L.; Yin, H.Y.; Xiao, E.T.; Sun, Z.L.; Li, A.Q. A kind of NiTi-wire shape memory alloy damper to simultaneously damp tension, compression and torsion. *Struct. Eng. Mech.* **2006**, *22*, 241–262. [[CrossRef](#)]
95. Qiu, C.X.; Wang, H.Y.; Liu, J.W.; Qi, J.; Wang, Y.M. Experimental tests and finite element simulations of a new SMA-steel damper. *Smart Mater. Struct.* **2020**, *29*, 035016. [[CrossRef](#)]
96. Ma, H.W.; Cho, C.D. Feasibility study on a superelastic SMA damper with re-centring capability. *Mater. Sci. Eng. A-Struct. Mater. Prop. Microstruct. Process.* **2008**, *473*, 290–296. [[CrossRef](#)]
97. Feng, W.K.; Fang, C.; Wang, W. Behavior and design of top flange-rotated self-centering steel connections equipped with SMA ring spring dampers. *J. Constr. Steel Res.* **2019**, *159*, 315–329. [[CrossRef](#)]
98. Sui, J.Y.; Xu, C.M.; Liu, W.F. Study of a new type sma damper. In Proceedings of the 1st International Conference on Civil Engineering, Architecture and Building Materials (CEABM 2011), Haikou, China, 18–20 June 2011; pp. 2897–2901.
99. Qiu, C.X.; Liu, J.W.; Du, X.L. Cyclic behavior of SMA slip friction damper. *Eng. Struct.* **2022**, *250*, 113407. [[CrossRef](#)]
100. Jia, Y.Q.; Wang, C.; Zhang, R.F.; Li, L.Z.; Lu, Z.D. A Double Shape Memory Alloy Damper for Structural Vibration Control. *Int. J. Struct. Stab. Dyn.* **2021**, *21*, 2150098. [[CrossRef](#)]
101. Fang, C.; Wang, W.; Ji, Y.Z.; Yam, M.C.H. Superior low-cycle fatigue performance of iron-based SMA for seismic damping application. *J. Constr. Steel Res.* **2021**, *184*, 106817. [[CrossRef](#)]
102. Miller, D.J.; Fahnestock, L.A.; Eatherton, M.R. Development and experimental validation of a nickel-titanium shape memory alloy self-centering buckling-restrained brace. *Eng. Struct.* **2012**, *40*, 288–298. [[CrossRef](#)]
103. Shi, F.; Zhou, Y.; Ozbulut, O.E.; Ren, F.M. Hysteretic response and failure behavior of an SMA cable-based self-centering brace. *Struct. Control Health Monit.* **2022**, *29*, e2847. [[CrossRef](#)]
104. Ozbulut, O.E.; Roschke, P.N.; Lin, P.Y.; Loh, C.H. GA-based optimum design of a shape memory alloy device for seismic response mitigation. *Smart Mater. Struct.* **2010**, *19*, 065004. [[CrossRef](#)]
105. Cao, S.S.; Ozbulut, O.E. Long-stroke shape memory alloy restrainers for seismic protection of bridges. *Smart Mater. Struct.* **2020**, *29*, 115005. [[CrossRef](#)]
106. Fang, C.; Chen, J.B.; Wang, W. SMA-braced steel frames influenced by temperature: Practical modelling strategy and probabilistic performance assessment. *J. Build. Eng.* **2023**, *76*. [[CrossRef](#)]
107. Qiang, X.H.; Wu, Y.P.; Wang, Y.H.; Jiang, X. Novel crack repair method of steel bridge diaphragm employing Fe-SMA. *Eng. Struct.* **2023**, *292*, 116548. [[CrossRef](#)]
108. Zheng, B.; Dawood, M. Fatigue Strengthening of Metallic Structures with a Thermally Activated Shape Memory Alloy Fiber-Reinforced Polymer Patch. *J. Compos. Constr.* **2017**, *21*, 04016113. [[CrossRef](#)]
109. Kean, V.; Chen, T.; Li, L.Z. Numerical study of fatigue life of SMA/CFRP patches retrofitted to central-cracked steel plates. *Constr. Build. Mater.* **2021**, *284*, 122845. [[CrossRef](#)]
110. Qiang, X.H.; Wu, Y.P.; Jiang, X.; Xu, G.W. Fatigue performance of cracked diaphragm cutouts in steel bridge reinforced employing CFRP/SMA. *J. Constr. Steel Res.* **2023**, *211*, 108136. [[CrossRef](#)]
111. Deng, J.; Fei, Z.Y.; Wu, Z.G.; Li, J.H.; Huang, W.Z. Integrating SMA and CFRP for fatigue strengthening of edge-cracked steel plates. *J. Constr. Steel Res.* **2023**, *206*, 107931. [[CrossRef](#)]
112. Vujtech, J.; Ryjacek, P.; Matos, J.C.; Ghafoori, E. Iron-Based Shape Memory Alloy Strengthening of a 113-Years Steel Bridge. In Proceedings of the 10th International Conference on Fibre-Reinforced Polymer (FRP) Composites in Civil Engineering (CICE), Istanbul, Turkey, 8–10 December 2021; pp. 2311–2321.
113. Deng, J.; Fei, Z.Y.; Li, J.H.; Huang, H.F. Flexural capacity enhancing of notched steel beams by combining shape memory alloy wires and carbon fiber-reinforced polymer sheets. *Adv. Struct. Eng.* **2023**, *26*, 1525–1537. [[CrossRef](#)]

114. Hosseinnajad, H.; Lotfollahi-Yaghin, M.A.; Hosseinzadeh, Y.; Maleki, A. Evaluating performance of the post-tensioned tapered steel beams with shape memory alloy tendons. *Earthq. Struct.* **2022**, *23*, 221–229. [[CrossRef](#)]
115. Hosseinnajad, H.; Lotfollahi-Yaghin, M.; Hosseinzadeh, Y.; Maleki, A. Numerical Investigation of Response of the Post-tensioned Tapered Steel Beams with Shape Memory Alloy Tendons. *Int. J. Eng.* **2021**, *34*, 782–792. [[CrossRef](#)]
116. Xing, D.J.; Yang, B.Q.; Wang, M.D. Design of SMA Damper and Analysis on Seismic Control of Frame Structure. In Proceedings of the International Conference on Civil, Architectural and Hydraulic Engineering (ICCAHE 2012), Zhangjiajie, China, 10–12 August 2012; pp. 2584–2589.
117. Li, R.; Ge, H.B.; Shu, G.P. Parametric Study on Seismic Control Design of a New Type of SMA Damper Installed in a Frame-Type Bridge Pier. *J. Aerosp. Eng.* **2018**, *31*, 04017100. [[CrossRef](#)]
118. Lv, H.W.; Huang, B. Vibration Reduction Performance of a New Tuned Mass Damper with Pre-Strained Superelastic SMA Helical Springs. *Int. J. Struct. Stab. Dyn.* **2023**, 2450047. [[CrossRef](#)]
119. Qiu, C.X.; Gong, Z.H.; Peng, C.L.; Li, H. Seismic vibration control of an innovative self-centering damper using confined SMA core. *Smart Struct. Syst.* **2020**, *25*, 241–254. [[CrossRef](#)]
120. Asgarian, B.; Moradi, S. Seismic response of steel braced frames with shape memory alloy braces. *J. Constr. Steel Res.* **2011**, *67*, 65–74. [[CrossRef](#)]
121. Jalalvandi, M.; Soraghi, A.; Farooghi-Mehr, S.M.; Haghollahi, A.; Abasi, A. Study and Comparison of the Performance of Steel Frames with BRB and SMA Bracing. *Struct. Eng. Int.* **2023**, *33*, 413–424. [[CrossRef](#)]
122. Fahiminia, M.; Zahrai, S.M. Seismic performance of simple steel frames with buckling-restrained knee braces & SMA to reduce residual displacement. *Soil Dyn. Earthq. Eng.* **2020**, *137*, 106268. [[CrossRef](#)]
123. Vafaei, D.; Eskandari, R. Seismic performance of steel mega braced frames equipped with shape-memory alloy braces under near-fault earthquakes. *Struct. Des. Tall Spec. Build.* **2016**, *25*, 3–21. [[CrossRef](#)]
124. Qiu, C.X.; Zhu, S.Y. Shake table test and numerical study of self-centering steel frame with SMA braces. *Earthq. Eng. Struct. Dyn.* **2017**, *46*, 117–137. [[CrossRef](#)]
125. Qiu, C.X.; Zhao, X.N.; Zhu, S.Y. Seismic upgrading of multistory steel moment-resisting frames by installing shape memory alloy braces: Design method and performance evaluation. *Struct. Control Health Monit.* **2020**, *27*, e2596. [[CrossRef](#)]

**Disclaimer/Publisher’s Note:** The statements, opinions and data contained in all publications are solely those of the individual author(s) and contributor(s) and not of MDPI and/or the editor(s). MDPI and/or the editor(s) disclaim responsibility for any injury to people or property resulting from any ideas, methods, instructions or products referred to in the content.